International Journal of Pharmaceutics 422 (2012) 332–337

Contents lists available at SciVerse ScienceDirect

International Journal of Pharmaceutics

journal homepage: www.elsevier.com/locate/ijpharm

Note

Gene delivery system involving Bubble liposomes and ultrasound for the efficient *in vivo* delivery of genes into mouse tongue tissue

Marika Sugano[a,b], Yoichi Negishi[b,*], Yoko Endo-Takahashi[b], Ryo Suzuki[c], Kazuo Maruyama[c], Matsuo Yamamoto[a,**], Yukihiko Aramaki[b]

[a] Department of Periodontology, Showa University School of Dentistry, 2-1-1 Kitasenzoku, Ohta-ku, Tokyo 145-8515, Japan
[b] Department of Drug Delivery and Molecular Biopharmaceutics, School of Pharmacy, Tokyo University of Pharmacy and Life Sciences, 1432-1 Horinouchi, Hachioji, Tokyo 192-0392, Japan
[c] Department of Biopharmaceutics, School of Pharmaceutical Sciences, Teikyo University, 1091-1 Suwarashi, Midori-ku, Sagamihara, Kanagawa 252-5195, Japan

ARTICLE INFO

Article history:
Received 16 August 2011
Received in revised form 25 October 2011
Accepted 2 November 2011
Available online 11 November 2011

Keywords:
Bubble liposomes
Ultrasound
Gene delivery
Tongue tissue

ABSTRACT

Oral squamous cell carcinoma is the most common type of head and neck cancer. Recently, efficient, easy, and minimally invasive gene delivery methods are expected to be developed as cancer gene therapies. However, the optimal method for delivering therapeutic genes into oral tissue for cancer treatment has not been elucidated. Therefore, we hypothesized that the tongue is a good target tissue for gene delivery with Bubble liposomes and ultrasound. To assess this, we attempted to deliver a mixture of plasmid DNA encoding a luciferase or enhanced green fluorescent protein, and Bubble liposomes into murine tongue with or without ultrasound exposure. The ultrasound conditions were 1 MHz, 2 W/cm^2, 60 s, and duty cycle: 50%. The time-course of gene expression in the tongue was investigated with a luciferase assay and fluorescent microscopy. Luciferase expression was significantly increased in tongue transfected using Bubble liposomes and ultrasound compared with that of the tongue untreated with ultrasound, and this high level of luciferase activity was maintained for 2 weeks. From these results, Bubble liposomes can be used in combination with ultrasound to efficiently deliver plasmid DNA into the tongue *in vivo*. This technique is a highly promising approach for gene delivery into oral tissue.

1. Introduction

Although the most common types of oral disease are dental caries and periodontal disease, oral cancer such as squamous cell carcinoma (SCC) is associated with an unfavorable prognosis. Tongue SCC is the most common type of oral SCC, and metastasis to the lymph nodes and/or proximal tissues often occurs (Ohba et al., 2010; Shiga et al., 2007). The current treatments for tongue SCC include surgery, radiation therapy, and chemotherapy, all of which have severe side effects. Therefore, cancer cell-specific treatment that does not damage normal cells is desired. Recently, gene delivery to tumor cells such as using adenovirus-based p53 gene therapies has gained attention (Edelman and Nemunaitis, 2003; Huang et al., 2009). The two main gene carrier systems for gene therapy are viral vectors and non-viral delivery systems. Viral vectors are efficient carriers for gene transfection (Lundstrom, 2003), but some serious problems such as immunogenicity and toxicity have been reported (Check, 2002, 2003; Marshall, 1999). On the other hand, the transfection efficiency of non-viral methods remains a problem. Therefore, it is necessary to develop a safe and highly efficient gene transfer method.

Recently, it has been reported that the use of microbubbles in combination with low energy ultrasound (US) enhances transfection efficiency (Greenleaf et al., 1998; Shohet et al., 2000; Sonoda et al., 2006; Taniyama et al., 2002a,b). Regarding the orofacial area, there have been a few reports about gene delivery using microbubbles and US, for example, Sakai et al. (2009) and Chen et al. (2009) reported transient gene transfection in the target tissue using different microbubbles. However, prolonged gene expression is necessary in the clinical setting, and the size and stability of the microbubbles employed also needs to be improved. Previously, we developed "Bubble liposomes (BL)" as a novel gene delivery carrier system and reported that gene delivery using a combination of BL and US is safer and more efficient in both *in vitro* and *in vivo* compared to other non-viral methods (Negishi et al., 2008, 2011; Suzuki et al., 2007). However, there are no reports about gene delivery to

Abbreviations: SCC, squamous cell carcinoma; US, ultrasound; BL, Bubble liposome; PEG, polyethylene glycol; EBD, Evans blue dye; QOL, quality of life.

* Corresponding author. Tel.: +81 42 676 3183; fax: +81 42 676 3182.
** Corresponding author. Tel: +81 3 5498 1995; fax: +81 3 3787 7886.
E-mail addresses: negishi@toyaku.ac.jp (Y. Negishi), yamamoto-m@dent.showa-u.ac.jp (M. Yamamoto).

0378-5173/$ – see front matter © 2011 Elsevier B.V. All rights reserved.
doi:10.1016/j.ijpharm.2011.11.001

oral tissue using this technique. Therefore, in the present study, we assessed whether efficient gene delivery into mouse tongue tissue could be achieved using BL and US.

2. Materials and methods

2.1. Animals

Five-week-old male ICR mice were used for all animal experiments (Tokyo Laboratory Animals Science, Tokyo, Japan). All studies were approved by the Animal Experiment Committee of Tokyo University of Pharmacy and Life Sciences. The mice were given feed and tap water *ad libitum* throughout the experimental period.

2.2. Preparation of Bubble liposomes

The BL were prepared using the previously described method (Negishi et al., 2008; Suzuki et al., 2007). In brief, PEG liposomes composed of 1,2-dipalmitoyl-sn-glycero-3-phosphocholine (DPPC) (NOF Corporation, Tokyo, Japan) and 1,2-distearoyl-sn-glycero-3-phosphatidyl-ethanolamine-polyethyleneglycol (DSPE-PEG_{2000}-OMe) (NOF Corporation) in a molar ratio of 94:6 were prepared using a reverse phase evaporation method. In brief, all reagents were dissolved in 1:1 (v/v) chloroform/diisopropyl ether. Phosphate-buffered saline was added to the lipid solution, and the mixture was sonicated and then evaporated at 47 °C. Then, the organic solvent was completely removed, and the size of the liposomes was adjusted to less than 200 nm using extruding equipment and a sizing filter (pore size: 200 nm) (Nuclepore Track-Etch Membrane, Whatman plc, UK). The lipid concentration was measured using a Phospholipid C test Wako (Wako Pure Chemical Industries Ltd., Osaka, Japan), and BL were prepared from liposomes and perfluoropropane gas (Takachio Chemical Ind. Co. Ltd., Tokyo, Japan). First, 2-mL sterilized vials containing 0.8 mL of a liposome suspension (lipid concentration: 1 mg/mL) were filled with perfluoropropane gas, capped, and then pressurized with a further 3 mL of perfluoropropane gas. The vial was placed in a bath-type sonicator (42 kHz, 100 W) (Bransonic 2510j-DTH, Branson Ultrasonics Co., Danbury, CT, USA) for 5 min to form BL.

2.3. Plasmid DNA

Two reporter plasmids were used. The pcDNA3-Luc plasmid, which is derived from pGL3-basic (Promega, Madison, WI), is an expression vector encoding the firefly luciferase gene under the control of the cytomegalovirus promoter. The pEGFP-N3 plasmid (Clontech Laboratories, Inc., Mountain View, CA) is an expression vector encoding enhanced green fluorescent protein (EGFP) under the control of the cytomegalovirus promoter.

2.4. In vivo gene delivery using BL and US

ICR mice were anesthetized with 10 mg/mL pentobarbital throughout each procedure. A 20 μL mixture of pDNA (20 μg) and BL (10 μg) was injected into the tongue tissue of the mice using a 33-gauge syringe (Hamilton Company, USA), and US exposure (frequency: 1 MHz; duty: 50%; intensity: 2 W/cm^2; time: 60 s) was immediately applied to the injection site. A Sonitron 2000 (Nepa Gene Co., Ltd.) was used as an ultrasound generator. Several days after the injection, the mice were sacrificed, and the tongue tissue in the US-exposed area was collected and homogenized with Polytron (Kinematica, Inc., New York, USA). The cell lysate and tissue homogenates were prepared with a lysis buffer (0.1 M Tris–HCl (pH 7.8), 0.1% Triton X-100, and 2 mM EDTA). Luciferase activity was then measured using a luciferase assay system (Promega, Madison, WI) and a luminometer (LB96V, Belthold Japan Co. Ltd., Tokyo, Japan). Activity is indicated as relative light units (RLU) per mg of protein. To analyze EGFP expression, the collected tongue was fixed with paraformaldehyde and dehydrated in sucrose solution. The specimens were then embedded in OCT compound and immediately frozen at −80 °C. Serial 10 μm thick sections were then cut using a cryostat and observed with a fluorescence microscope (Axiovert 200 M, Carl Zeiss).

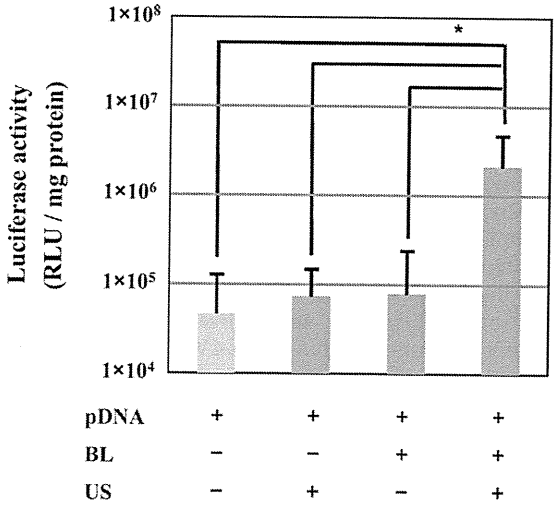

Fig. 1. Luciferase activity in tongue tissue transfected with a reporter gene using BL and US. Mice were subjected to BL and US-mediated luciferase gene transfer. Relative luciferase activity was determined on day 5 after transfection. The data are shown as the mean ± S.D. *$P < 0.05$, Mann–Whitney's U test ($n = 5$), compared to other groups. pDNA (pCMV-luciferase): 20 μg; BL: 10 μg; US conditions: frequency: 1 MHz, duty: 50%, and intensity: 2 W/cm^2, time: 60 s. BL, Bubble liposomes; US, ultrasound.

2.5. Tissue damage testing using Evans blue dye (EBD)

Tissue-damage testing using EBD was performed as reported previously (Liu and Huang, 2002). Briefly, EBD was dissolved in PBS (10 mg/mL) and sterilized using 0.2 μm membrane filters. The mice treated with pDNA, BL, and US were administered EBD (0.5 mg dye/10 g body weight) by tail vein injection and then sacrificed 1 day after the EBD injection. Their tongue tissues were collected, fixed with paraformaldehyde, embedded in OCT compound, and immediately frozen at −80 °C. Serial 10 μm thick sections were cut using a cryostat and observed with a fluorescence microscope (Axiovert 200 M, Carl Zeiss).

2.6. Statistical analysis

All data are shown as the mean ± S.D. ($n = 5$ or 6). Mann–Whitney's U test was used to determine the statistical significance of any differences. The differences detected in multiple comparison tests were assessed by two-way repeated-measures analysis of variance (ANOVA). Differences associated with a $P < 0.05$ were considered significant.

3. Results

We first tried to deliver naked pDNA into tongue tissue using BL and US under the conditions used in a previous study, in which naked pDNA was delivered into skeletal muscles (Negishi et al., 2011). Significantly increased gene expression was detected in the group treated with BL and US exposure (Fig. 1.); i.e., it was 12-fold higher than that of the group treated with pDNA alone. In the groups

treated with pDNA + BL and pDNA + US, the relative luciferase activity remained as low as that of the pDNA alone group.

Then, to optimize the conditions for *in vivo* gene delivery into tongue tissue, we examined three transfection condition parameters, the total pDNA, US intensity, and US exposure time. First, to assess whether the pDNA injection volume affected transfection efficiency, we adjusted it from 0.2 μg to 20 μg. As a result, the increase in luciferase activity was found to be dependent on the amount of pDNA, and the most significant increase in relative luciferase activity was detected at 20 μg pDNA (Fig. 2a.). Next, we investigated the relationship between US intensity and the transfection efficiency of gene delivery into tongue tissue. The US intensity was varied within the 0–4 W/cm^2 range. The relative luciferase activity was significantly higher in the groups treated with US intensities of 2.0 W/cm^2 and 4.0 W/cm^2 (Fig. 2b.). Moreover, we also examined the effect of the US exposure time and found that luciferase activity was highest when US was delivered for 60 s (Fig. 2c.). In contrast, when US was delivered for a longer period, the transfection efficiency tended to decrease. We further examined the duration of gene expression induced after treatment with BL and US exposure. As a result, we found that high luciferase activity was maintained for about 2 weeks (Fig. 3).

Next, the localization of EGFP-expressing cells and tissue damage after gene delivery with BL and US was observed with fluorescence microscopy. In histological observations, distinct EGFP expression was observed in the tongue tissue treated with BL and US (Fig. 4.). In the group treated with BL and US, there were many EGFP expressing cells throughout the muscle layer. In the other groups, only a few sporadically distributed cells were found to express EGFP. However, using a high US intensity to achieve efficient gene transfection leads to tissue damage (Duvshani-Eshet and Machluf, 2005; Kim et al., 1996). Therefore, to investigate the tissue damage caused by gene transfection, mice had EBD injected into their tail veins one day before they were euthanized, as enhanced EBD uptake indicates increased cell damage. As a result, we found that severe tissue damage was observed after the application of high intensity US (4.0 W/cm^2) or a US exposure time of 120 s or more (Fig. 5).

From these results, we suggest that the optimal conditions for gene delivery into the murine tongue using BL and US are as follows: total pDNA (2 μg/μL): 20 μg, US intensity: 2 W/cm^2, and US exposure time: 60 s.

In addition, *Sonazoid*™, a commercially available microbubble, has been used as an echo-contrast gas in clinical. We therefore also test the transfection efficacy of *Sonazoid*™ in the same experiment. However, the luciferase activity was moderate increase even in the combination of US exposure (data not shown).

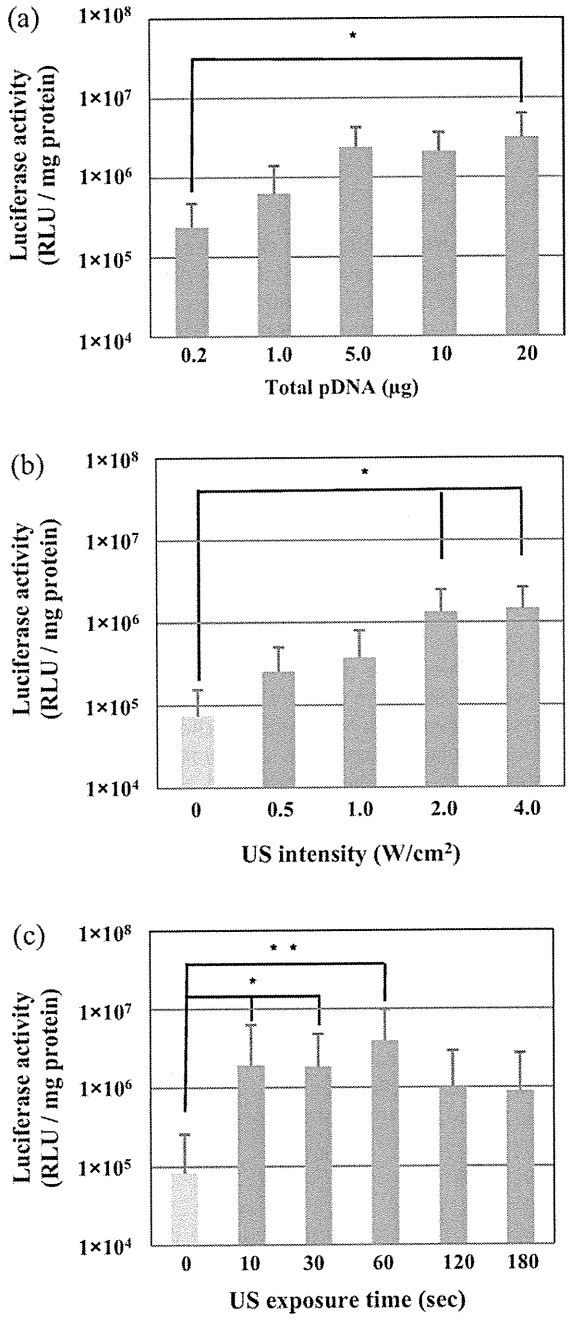

Fig. 2. Characteristics of ultrasound gene delivery systems using BL. To examine the optimal parameters for BL and US-mediated gene transfer into tongue tissue, the mice were subjected to various transfection conditions; i.e., by altering the amount of pDNA, US intensity, and US exposure time. The other conditions were as follows: US frequency: 1 MHz, duty: 50%. The data are shown as the mean ± S.D. (a) The variation in the gene expression level induced by changing the amount of pDNA. The amount of pDNA was changed from 0.2 μg to 20 μg. The total injection volume remained constant at 20 μL. *$P < 0.05$, Mann–Whitney's U test ($n = 5$), compared with 0.2 μg of pDNA. (b) The variation in the gene expression level induced by changes in the US intensity. The US intensity was set at 0, 0.5, 1.0, 2.0, or 4.0 W/cm^2. *$P < 0.05$, Mann–Whitney's U test ($n = 5$), compared with 0 W/cm^2 (no US exposure). (c) The variation in the gene expression level induced by changes in the US exposure time. The US duration was set at 0, 10, 30, 60, 120, or 180 s. *$P < 0.05$, **$P < 0.01$, Mann–Whitney's U test ($n = 6$), compared with 0 s (no US exposure).

4. Discussion

Gene therapy is expected to be clinically useful for treating genetic diseases, cancer, and/or infectious diseases. These diseases are also found in the orofacial area, and a number of studies have recently examined the usefulness of gene therapy for a variety of oral diseases. In those studies, gene delivery into the orofacial area was performed with viral vectors due to their high transfection efficiency. For example, it has been reported that reporter genes were transfected into rat salivary glands using several kinds of viral vector (Shai et al., 2002; Zheng and Baum, 2005). In addition, viruses are the most common transfer system used to deliver gene therapy to oral SCC (Ladeinde et al., 2005). However, viral systems are not perfect because of their safety and immunogenicity (Check, 2002, 2003; Marshall, 1999).

Therefore, many researchers have tried to establish non-viral gene delivery systems that combine high transfection efficiency with reduced invasiveness. Among these non-viral gene delivery methods, Fechheimer et al. (1987) first reported the US-mediated gene delivery technique, and since then gene transfer using ultrasonic waves has developed into a safe and non-viral gene transfection technology. A physical phenomenon known as

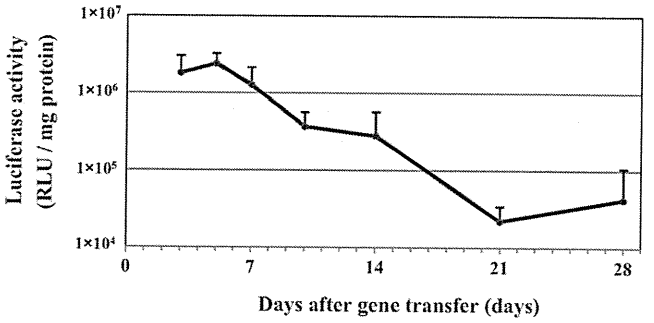

Fig. 3. Time-dependent changes in luciferase activity in tongue tissue transfected using BL and US. Relative luciferase activity was examined at 3, 5, 7, 10, 14, 21, and 28 days after the gene transfection. The transfection conditions were as follows: pDNA (pCMV-luciferase): 20 μg; BL: 10 μg; US conditions: frequency: 1 MHz, duty: 50%, intensity: 2 W/cm², and time: 60 s. The data are shown as the mean ± S.D.

cavitation is assumed to be the mechanism responsible for US-mediated gene delivery. When the "cavitation bubble" generated by US energy is destroyed, it produces a jet stream, which in turn produces transient pores in cell membranes, allowing extracellular plasmid DNA to enter the cytosol. In addition, it has been shown that transfection efficiency often improves in the presence of microbubbles, and the utility of their application has been demonstrated both *in vitro* and *in vivo* (Greenleaf et al., 1998; Shohet et al., 2000; Sonoda et al., 2006; Taniyama et al., 2002a,b).

Microbubbles were originally used as an ultrasonic contrast agent for clinical ultrasound diagnosis. A variety of microbubbles with different encapsulated gas types, shell materials, and diluents have been designed. The mean diameter of microbubbles that are marketed as echo-enhanced contrast agents is several micrometers. Several reports have compared the transfection efficiencies of these microbubbles during their use in combination with US (Alter et al., 2009; Hassan et al., 2009; Li et al., 2003; Wang et al., 2005).

However, the intravascular application of microbubbles is hindered by problems with their stability, targeting ability, and particle size. Thus, we developed and applied a new liposome composed of hydrophilic polyethylene glycol (PEG) as a drug delivery system. PEG-liposomes containing perfluoropropane gas are known as "Bubble liposomes (BL)". We have reported that this BL-mediated US gene transfer system enhances transfection efficiency both *in vitro* and *in vivo* (Negishi et al., 2008, 2010; Suzuki et al., 2007, 2008a,b, 2010). Negishi et al. (2011) used gene transfer methods involving BL and US to transfect genes into murine skeletal muscle and discussed their reasons for selecting skeletal muscle as a target tissue for gene therapy. They stated that as skeletal muscle cells are large and display stability and longevity, they are an attractive target tissue for gene therapy.

The generation and oscillation of "cavitation bubbles" after ultrasound exposure is influenced by the composition and pressure of the organs surrounding the transfection site. Therefore, it is important to optimize each transfection condition in the targeted tissue. The majority of tongue tissue is composed of skeletal muscle and is covered with a keratinized oral mucosa. In our histological observations, distinct EGFP expression was observed in the tongue muscle, as shown in Fig. 4. On the other hand, scattered EGFP expression was observed on the surface area of the mucoepithelial layer (data not shown). Moreover, a previous report described that repeated US exposure enhances transfection efficiency and prolonged gene expression compared with single US exposure (Bekeredjian et al., 2003). In this study, we showed that high luciferase activity was maintained for 2 weeks in murine tongue tissue treated with BL and single US exposure. Such persistent expression is thought to be suitable for therapy against tongue cancer. Whether the effect of the therapeutic gene needs to be continuous depends on the disease being targeted; for example, whether it is an infectious or genetic disease. Therefore, if the gene delivery method involving BL and US is to be applied to other oral tissues, it is very important to optimize the transfection conditions for long-term gene expression in the target tissue. Further

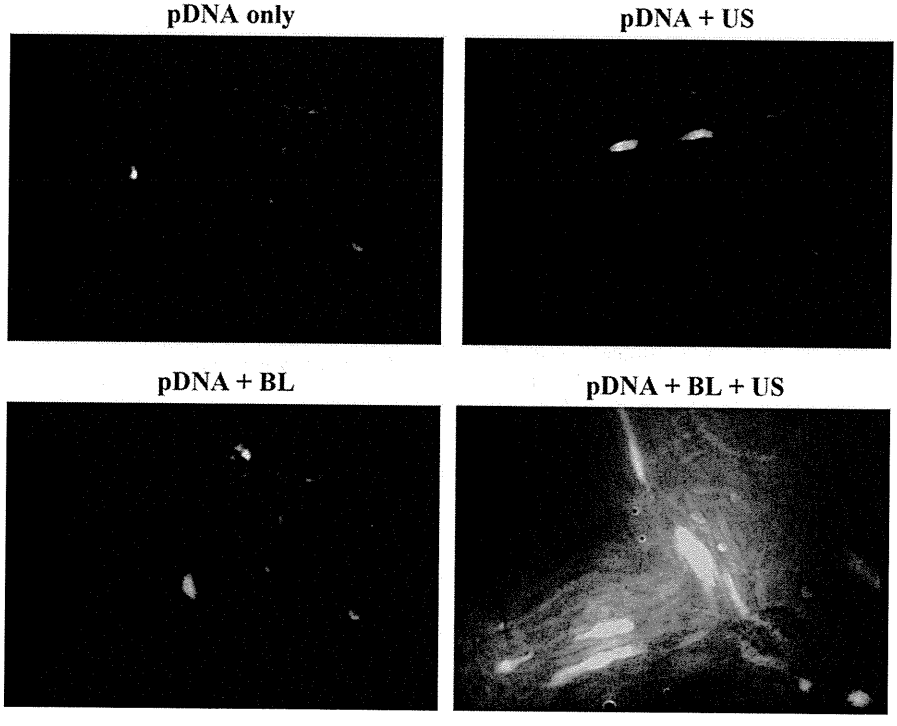

Fig. 4. EGFP expression in tongue tissue transfected with a reporter gene using BL and US. Mice were treated with BL and then subjected to US-mediated EGFP transfer into the tongue. On day 5 after the transfection, the tongue was sectioned into 10 μm thick slices using a cryostat, and EGFP expression was analyzed by fluorescent microscopy. Each of the gene transfer conditions is indicated above the pictures. Magnification: 200×. BL, Bubble liposomes; US, ultrasound.

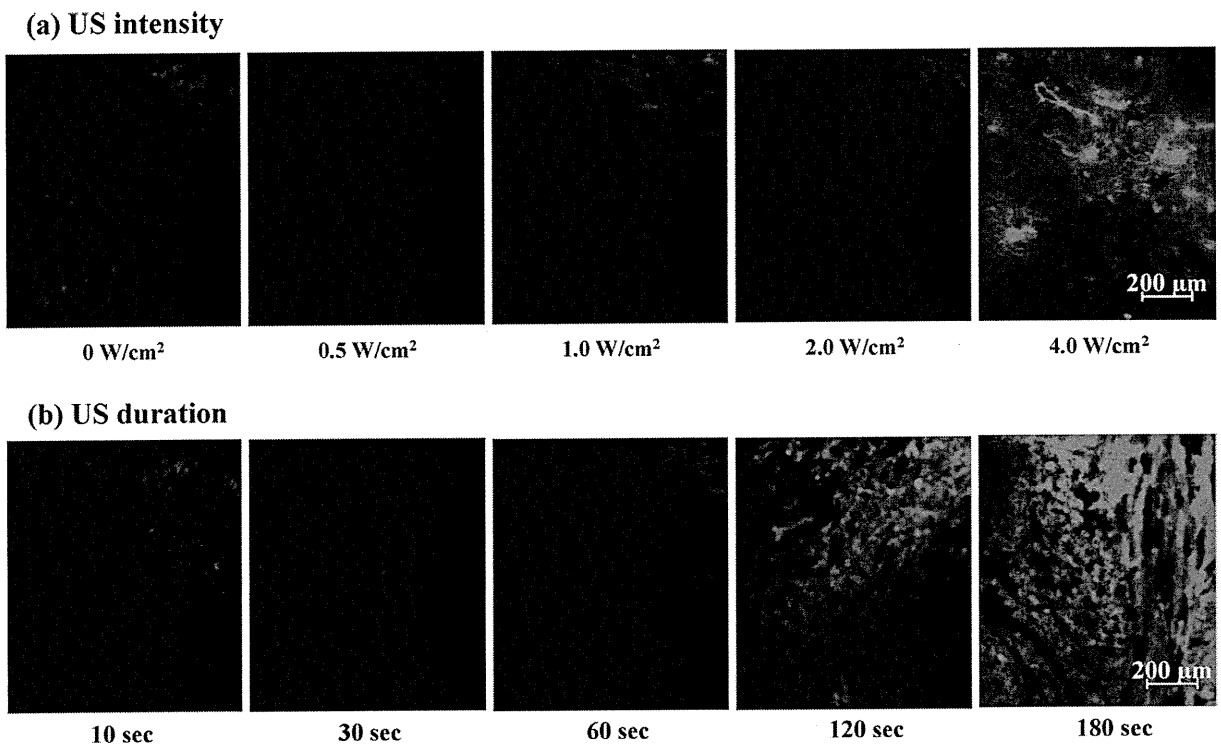

Fig. 5. Tissue-damage testing using EBD. To assess the tissue-damage by BL and US-mediated gene transfer into tongue tissue, the mice were treated pDNA with BL and various US exposure conditions. (a) At a frequency of 1 MHz with an intensity of 0, 0.5, 1.0, 2.0, or 4.0 W/cm² for 60 s (upper section). (b) At a frequency of 1 MHz with an intensity of 2.0 W/cm² for 10, 30, 60, 120, or 180 s (lower). Evans-blue fluorescence of 10 μm cryosections from the tongue was examined with fluorescence microscopy. Scale bar: 200 μm.

experiments using genes that encode therapeutic proteins are required to assess the clinical application of this US-mediated BL method.

This is the first report regarding gene transfer to tongue tissue using BL and US as a therapeutic method for diseases of the oral cavity. As mentioned above, tongue SCC is one of the most common forms of head and neck cancer; nevertheless, no standardized treatment strategy for this condition has been established (Shiga et al., 2007). Oral dysfunction and decreased quality of life (QOL) are often seen after surgical treatment in tongue SCC patients. Therefore, gene delivery systems involving BL and US exposure that enable cancer cell-specific treatment may improve the QOL of tongue SCC patients.

5. Conclusion

In conclusion, the results of this study suggest that our gene delivery method involving BL and US could be a useful treatment for patients with tongue SCC. This US-mediated BL technique is a highly promising approach for gene delivery into oral tissue.

Acknowledgements

We are grateful to Dr. Katsuro Tachibana (Department of Anatomy, School of Medicine, Fukuoka University) for technical advice regarding the induction of cavitation with US, and to Mr. Yasuhiko Hayakawa and Mr. Kosho Suzuki (Nepa Gene Co., Ltd.) for technical advice regarding US exposure. This study was supported in part by the Industrial Technology Research Grant Program (04A05010) from New Energy, the Industrial Technology Development Organization (NEDO) of Japan.

References

Alter, J., Sennoga, C.A., Lopes, D.M., Eckersley, R.J., Wells, D.J., 2009. Microbubble stability is a major determinant of the efficiency of ultrasound and microbubble mediated in vivo gene transfer. Ultrasound Med. Biol. 35, 976–984.
Bekeredjian, R., Chen, S., Frenkel, P.A., Grayburn, P.A., Shohet, R.V., 2003. Ultrasound-targeted microbubble destruction can repeatedly direct highly specific plasmid expression to the heart. Circulation 108, 1022–1026.
Check, E., 2002. Safety panel backs principle of gene-therapy trials. Nature 420, 595.
Check, E., 2003. Second cancer case halts gene-therapy trials. Nature 421, 305.
Chen, R., Chiba, M., Mori, S., Fukumoto, M., Kodama, T., 2009. Periodontal gene transfer by ultrasound and nano/microbubbles. J. Dent. Res. 88, 1008–1013.
Duvshani-Eshet, M., Machluf, M., 2005. Therapeutic ultrasound optimization for gene delivery: a key factor achieving nuclear DNA localization. J. Control. Release 108, 513–528.
Edelman, J., Nemunaitis, J., 2003. Adenoviral p53 gene therapy in squamous cell cancer of the head and neck region. Curr. Opin. Mol. Ther. 5, 611–617.
Fechheimer, M., Boylan, J.F., Parker, S., Sisken, J.E., Patel, G.L., Zimmer, S.G., 1987. Transfection of mammalian cells with plasmid DNA by scrape loading and sonication loading. Proc. Natl. Acad. Sci. U.S.A. 84, 8463–8467.
Greenleaf, W.J., Bolander, M.E., Sarkar, G., Goldring, M.B., Greenleaf, J.F., 1998. Artificial cavitation nuclei significantly enhance acoustically induced cell transfection. Ultrasound Med. Biol. 24, 587–595.
Hassan, M.A., Feril Jr., L.B., Suzuki, K., Kudo, N., Tachibana, K., Kondo, T., 2009. Evaluation and comparison of three novel microbubbles: enhancement of ultrasound-induced cell death and free radicals production. Ultrason. Sonochem. 16, 372–378.
Huang, P.I., Chang, J.F., Kirn, D.H., Liu, T.C., 2009. Targeted genetic and viral therapy for advanced head and neck cancers. Drug Discov. Today 14, 570–578.
Kim, H.J., Greenleaf, J.F., Kinnick, R.R., Bronk, J.T., Bolander, M.E., 1996. Ultrasound-mediated transfection of mammalian cells. Hum. Gene Ther. 7, 1339–1346.
Ladeinde, A.L., Ogunlewe, M.O., Adeyemo, W.L., Bamgbose, B.O., 2005. Gene therapy in the management of oral cancer: a review of recent developments. Niger. Postgrad. Med. J. 12, 18–22.
Li, T., Tachibana, K., Kuroki, M., 2003. Gene transfer with echo-enhanced contrast agents: comparison between Albunex, Optison, and Levovist in mice – initial results. Radiology 229, 423–428.
Liu, F., Huang, L., 2002. A syringe electrode device for simultaneous injection of DNA and electrotransfer. Mol. Ther. 5, 323–328.
Lundstrom, K., 2003. Latest development in viral vectors for gene therapy. Trends Biotechnol. 21, 117–122.
Marshall, E., 1999. Gene therapy death prompts review of adenovirus vector. Science 286, 2244–2245.

Negishi, Y., Endo, Y., Fukuyama, T., Suzuki, R., Takizawa, T., Omata, D., Maruyama, K., Aramaki, Y., 2008. Delivery of siRNA into the cytoplasm by liposomal bubbles and ultrasound. J. Control. Release 132, 124–130.

Negishi, Y., Matsuo, K., Endo-Takahashi, Y., Suzuki, K., Matsuki, Y., Takagi, N., Suzuki, R., Maruyama, K., Aramaki, Y., 2011. Delivery of an angiogenic gene into ischemic muscle by novel Bubble liposomes followed by ultrasound exposure. Pharm. Res. 28, 712–719.

Negishi, Y., Omata, D., Iijima, H., Takabayashi, Y., Suzuki, K., Endo, Y., Suzuki, R., Maruyama, K., Nomizu, M., Aramaki, Y., 2010. Enhanced laminin-derived peptide AG73-mediated liposomal gene transfer by Bubble liposomes and ultrasound. Mol. Pharmacol. 7, 217–226.

Ohba, T., Motoi, N., Kimura, Y., Okumura, S., Kawabata, K., Yoshizawa, Y., Inase, N., Ishikawa, Y., 2010. Cytokeratin expression profiling is useful for distinguishing between primary squamous cell carcinoma of the lung and pulmonary metastases from tongue cancer. Pathol. Int. 60, 575–580.

Sakai, T., Kawaguchi, M., Kosuge, Y., 2009. siRNA-mediated gene silencing in the salivary gland using in vivo microbubble-enhanced sonoporation. Oral Dis. 15, 505–511.

Shai, E., Falk, H., Honigman, A., Panet, A., Palmon, A., 2002. Gene transfer mediated by different viral vectors following direct cannulation of mouse submandibular salivary glands. Eur. J. Oral Sci. 110, 254–260.

Shiga, K., Ogawa, T., Sagai, S., Kato, K., Kobayashi, T., 2007. Management of the patients with early stage oral tongue cancers. Tohoku J. Exp. Med. 212, 389–396.

Shohet, R.V., Chen, S., Zhou, Y.T., Wang, Z., Meidell, R.S., Unger, R.H., Grayburn, P.A., 2000. Echocardiographic destruction of albumin microbubbles directs gene delivery to the myocardium. Circulation 101, 2554–2556.

Sonoda, S., Tachibana, K., Uchino, E., Okubo, A., Yamamoto, M., Sakoda, K., Hisatomi, T., Sonoda, K.H., Negishi, Y., Izumi, Y., Takao, S., Sakamoto, T., 2006. Gene transfer to corneal epithelium and keratocytes mediated by ultrasound with microbubbles. Invest. Ophthalmol. Vis. Sci. 47, 558–564.

Suzuki, R., Namai, E., Oda, Y., Nishiie, N., Otake, S., Koshima, R., Hirata, K., Taira, Y., Utoguchi, N., Negishi, Y., Nakagawa, S., Maruyama, K., 2010. Cancer gene therapy by IL-12 gene delivery using liposomal bubbles and tumoral ultrasound exposure. J. Control. Release 142, 245–250.

Suzuki, R., Takizawa, T., Negishi, Y., Hagisawa, K., Tanaka, K., Sawamura, K., Utoguchi, N., Nishioka, T., Maruyama, K., 2007. Gene delivery by combination of novel liposomal bubbles with perfluoropropane and ultrasound. J. Control. Release 117, 130–136.

Suzuki, R., Takizawa, T., Negishi, Y., Utoguchi, N., Maruyama, K., 2008a. Effective gene delivery with novel liposomal bubbles and ultrasonic destruction technology. Int. J. Pharm. 354, 49–55.

Suzuki, R., Takizawa, T., Negishi, Y., Utoguchi, N., Sawamura, K., Tanaka, K., Namai, E., Oda, Y., Matsumura, Y., Maruyama, K., 2008b. Tumor specific ultrasound enhanced gene transfer in vivo with novel liposomal bubbles. J. Control. Release 125, 137–144.

Taniyama, Y., Tachibana, K., Hiraoka, K., Aoki, M., Yamamoto, S., Matsumoto, K., Nakamura, T., Ogihara, T., Kaneda, Y., Morishita, R., 2002a. Development of safe and efficient novel nonviral gene transfer using ultrasound: enhancement of transfection efficiency of naked plasmid DNA in skeletal muscle. Gene Ther. 9, 372–380.

Taniyama, Y., Tachibana, K., Hiraoka, K., Namba, T., Yamasaki, K., Hashiya, N., Aoki, M., Ogihara, T., Yasufumi, K., Morishita, R., 2002b. Local delivery of plasmid DNA into rat carotid artery using ultrasound. Circulation 105, 1233–1239.

Wang, X., Liang, H.D., Dong, B., Lu, Q.L., Blomley, M.J., 2005. Gene transfer with microbubble ultrasound and plasmid DNA into skeletal muscle of mice: comparison between commercially available microbubble contrast agents. Radiology 237, 224–229.

Zheng, C., Baum, B.J., 2005. Evaluation of viral and mammalian promoters for use in gene delivery to salivary glands. Mol. Ther. 12, 528–536.

Journal of Drug Targeting, 2011, 1–7, Early Online

ISSN 1061-186X print/ISSN 1029-2330 online
DOI: 10.3109/1061186X.2011.585428

informa
healthcare

RESEARCH ARTICLE

Development of novel nucleic acid-loaded Bubble liposomes using cholesterol-conjugated siRNA

Yoichi Negishi[1], Yoko Endo-Takahashi[1], Kazumi Ishii[1], Ryo Suzuki[2], Yukiko Oguri[1], Takashi Murakami[3], Kazuo Maruyama[2], and Yukihiko Aramaki[1]

[1]*Department of Drug and Gene Delivery System, School of Pharmacy, Tokyo University of Pharmacy and Life Sciences, Tokyo, Japan,* [2]*Department of Biopharmaceutics, School of Pharmaceutical Sciences, Teikyo University, Kanagawa, Japan, and* [3]*Division of Bioimaging Sciences, Center for Molecular Medicine, Jichi Medical University, Tochigi, Japan*

Abstract

Recently, we developed polyethyleneglycol (PEG)-modified liposomes (Bubble liposomes; BLs) entrapping ultrasound (US) gas and reported that the combination of BLs and US exposure was an effective tool for the delivery of siRNA directly into cells and US-exposed tissues within a short period; however, the results were obtained using a mixture of BLs and naked siRNA. With systemic injections, it is important to control the biodistribution of both BLs and siRNA. In addition, the delivery of siRNA is affected by nuclease degradation and rapid removal from the circulation after intravenous administration. In this study, we attempted to prepare novel siRNA-loaded BLs (chol-si-BLs) using cholesterol-conjugated siRNA (chol-siRNA). We demonstrated that chol-siRNA could be loaded into BLs, leading to the stability of siRNA even in the presence of an RNase. The specific gene-silencing effect was also achieved by transfection with chol-si-BLs and US. Thus, the combination of chol-si-BLs with US exposure is expected to deliver siRNA into a specific tissue via systemic injection.

Keywords: siRNA delivery, ultrasound, microbubbles, chol-siRNA

Introduction

Recently, a combination of microbubbles and ultrasound (US) has been proposed as a less invasive and tissue-specific method of gene delivery. This combination produces transient changes in the permeability of the cell membrane and allows for the site-specific intracellular delivery of molecules such as dextran, pDNA, peptides, and siRNA both *in vitro* and *in vivo* (Taniyama et al., 2002a,b; Li et al., 2003; Unger et al., 2004; Kinoshita and Hynynen, 2005; Tsunoda et al., 2005; Sonoda et al., 2006); however, as existing microbubbles have issues with size, stability, and targeting function.

Polyethyleneglycol (PEG)-modified liposomes have excellent biocompatibility, stability, and a long circulation time, and can be easily prepared in a variety of sizes and modified to add a targeting function. For these reasons, they are widely used as carriers of drugs, antigens, and genes (Blume et al., 1990; Allen et al., 1991; Maruyama et al., 1992, 2004; Harata et al., 2004); therefore, PEG-liposomes containing a US-imaging gas could be used as novel gene delivery agents. We recently reported that "Bubble liposomes" (BLs) were suitable for gene delivery *in vitro* and *in vivo* (Suzuki et al., 2007, 2008a,b). Furthermore, we showed that BLs with US exposure was an effective tool for the delivery of siRNA *in vitro* and *in vivo* (Negishi et al., 2008); however, the results were obtained using a mixture of BLs and naked siRNA. With systemic injections, transfection efficiency is reduced if the BLs and siRNA are not colocalized in blood vessels; therefore, it is important to control the biodistribution of BLs and siRNA. In addition, siRNA is susceptible to nuclease degradation and rapid removal from the circulation after intravenous administration. In this study, we prepared siRNA-loaded BLs (chol-si-BLs) using cholesterol-conjugated siRNA (chol-siRNA) to overcome these issues. We also

Address for Correspondence: Yoichi Negishi, Department of Drug and Gene Delivery System, School of Pharmacy, Tokyo University of Pharmacy and Life Sciences, 1432-1 Horinouchi, Hachioji, Tokyo 192-0392, Japan. Tel and Fax: +81-42-676-3183. E-mail: negishi@toyaku.ac.jp
The first three authors contributed equally to this work

(Received 20 February 2011; revised 08 April 2011; accepted 17 April 2011)

investigated the stability of chol-siRNA in the presence of RNase and the gene-silencing effects of transfection with chol-si-BLs and US.

Methods

Cell lines and cultures

COS-7 cells were cultured in Dulbecco's modified Eagle's medium (DMEM; Kohjin Bio Co., Ltd., Tokyo, Japan) supplemented with 10% heat-inactivated fetal bovine serum (FBS; Equitech Bio Inc., Kerrville, TX), 100 units/mL penicillin and 100 μg/mL streptomycin in a humidified atmosphere containing 5% CO_2 at 37°C. Colon26 cells stably expressing firefly luciferase (Colon26-Luc) were cultured in DMEM supplemented with 10% heat-inactivated FBS, 100 units/mL penicillin, 100 μg/mL streptomycin and 10 μg/mL puromycin in a humidified atmosphere containing 5% CO_2 at 37°C.

Preparation of liposomes and BLs

To prepare liposomes for conventional BLs, 1,2-dipalmitoyl-sn-glycero-phosphatidylcholine and 1,2-distearoylphosphatidylethanolamine-methoxy-polyethylene glycol (PEG_{2000}) were mixed at a molar ratio of 94:6. Both lipids were purchased from NOF Corporation (Tokyo, Japan). For the preparation of chol-si-BLs, an adequate amount of chol-siRNA was added to the lipid mixture. Liposomes were prepared by a reverse-phase evaporation method (REV method) as described previously (Negishi et al., 2008). In brief, all reagents were added to the solution of 1:1 (v/v) chloroform/diisopropylether. Phosphate-buffered saline was added to the lipid solution and the mixture was sonicated and then evaporated at 47°C. The organic solvent was completely removed, and the size of the liposomes was adjusted to less than 200 nm using extruding equipment and a sizing filter (Nuclepore Track-Etch Membrane, 200 nm pore size; Whatman plc, UK). After being sized, the liposomes were passed through a sterile 0.45-μm syringe filter (Asahi Techno Glass Co., Chiba, Japan) for sterilization. To remove non-entrapped chol-siRNA, the liposomes were centrifuged twice at 1,00,000*g* for 1 h. The lipid concentration was measured using the phospholipid C test (Wako Pure Chemical Industries, Ltd., Osaka, Japan). BLs were prepared from liposomes and perfluoropropane gas (Takachiho Chemical Inc. Co., Ltd., Tokyo, Japan). First, 5-mL sterilized vials containing 2-mL liposome suspension (lipid concentration: 1 mg/mL) were filled with perfluoropropane gas, capped, and then pressured with 7.5 mL perfluoropropane gas. The vials were placed in a bath-type sonicator (42 kHz, 100 W, Bransonic 2510J-DTH; Branson Ultrasonics Co., Danbury, CT) for 5 min to form BLs. The zeta potential and mean size of the BLs were determined using light scattering method with a zeta potential/particle sizer, (Nicomp 380ZLS, Santa Barbara, CA). Fluorescein isothiocyanate (FITC)-labeled siRNA and flow cytometry were used to examine the interaction between siRNA and BLs. The fluorescence intensity of chol-si-BLs was analyzed using a FACSCanto (Becton Dickinson, San Jose, CA).

Plasmid DNA and siRNA

The plasmid pCMV-GL3, derived from pGL3-basic (Promega, Madison, WI), is an expression vector encoding the firefly luciferase gene under the control of a cytomegalovirus promoter. Small interfering RNA targeting luciferase (siLuc) and a random control siRNA (siRandom) were modified with cholesterol (chol) at the 3′ end of the sense strand (Japan Bio Services Co., Ltd., Saitama, Japan). Their sequences were as follows: siLuc, sense: 5′-GAACUGUGUGUGAGAGGUCCU*chol-3′, and antisense: 5′-AGGACCUCUCACACACAGUUc*g*C-3′; siRandom, sense: 5′-AGCUAGUCGUAGUGGAUGCGU*chol-3′ and antisense: 5′-ACGCAUCCACUACGACUAGCUc*g*C-3′. Lower-case letters represent 2′-*O*-methyl-modified nucleotides; asterisks represent phosphorothioate linkages. For some experiments, siRNA with FITC label at the 5′-end of the antisense strand was used.

Stability of siRNA in serum

The chol-siRNA and chol-si-BLs were incubated in 0–5% RNase for 30 min. After incubation, chol-siRNA was extracted by phenol chloroform isoamyl alcohol. The stability of siRNA was confirmed by 20% acrylamide gel electrophoresis. The gel was stained with SYBER SAFE (Invitrogen Japan K.K., Tokyo, Japan) and visualized under ultraviolet light.

Transfection of siRNA and/or pDNA into cells using BLs or chol-si-BLs

COS-7 cells (3×10^4 cells/well) were seeded into the wells of a 48-well plate (Asahi Techno Glass Co., Chiba, Japan) on the day before transfection. Colon26-Luc cells (3×10^4 cells) were suspended in a tube on the day of transfection. Five micrograms of pDNA and 60 μg chol-si-BLs were mixed together with culture medium containing 10% FBS and added to the cells. The cells were immediately exposed to US (frequency, 2 MHz; duty, 50%; burst rate, 2.0 Hz; intensity, 2.5 W/cm²) for 10 s through a 6-mm diameter probe placed in the well. A Sonopore 3000 (NEPA GENE, Co., Ltd., Chiba, Japan) was used to generate the US. The cells were washed twice with culture medium and cultured for 2 days.

To measure luciferase activity after transfection, cell lysate was prepared with a lysis buffer (0.1M Tris–HCl (pH 7.8), 0.1% Triton X-100, and 2 mM EDTA). Luciferase activity was measured using a luciferase assay kit (Promega, Madison, WI) and a luminometer (LB96V; Belthold Japan Co., Ltd., Tokyo, Japan). Activity was standardized as relative light units per mg of protein.

Statistical analyses

All data are the mean ± SD ($n = 4$). Data were considered significant when $P < 0.05$. The *t*-test was used to calculate statistical significance.

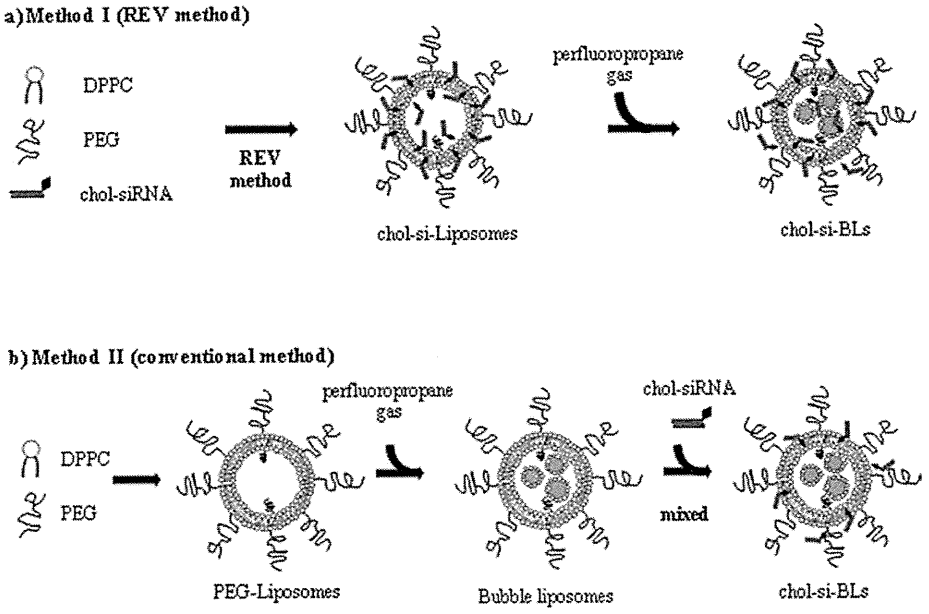

Figure 1. Scheme of chol-si-BLs prepared by two methods. (A) Method I; adding chol-siRNA to the lipid mixture and preparing liposomes by a REV method. (B) Method II; simply mixing BLs prepared by the conventional method and chol-siRNA.

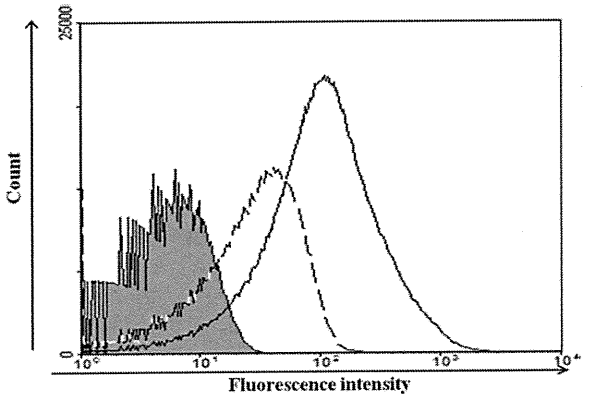

Figure 2. Interaction of chol-siRNA with BLs. The interaction was examined by analyzing a solution of chol-si-BLs with FACSCanto. Gray area: BLs only; solid line: chol-si-BLs prepared by Method I; dashed line: chol-si-BLs prepared by Method II; dotted line: chol-FITC-siRNA only.

Results

Preparation of chol-si-BLs

Initial experiments were performed to investigate the optimal method of preparation of chol-si-BLs (Figure 1). We attempted to add chol-siRNA to the lipid mixture, prepare liposomes by a REV method, and prepare BLs (Method I). We also attempted another method, that is, adding chol-siRNA to BLs prepared by the conventional method and mixing gently (Method II). To assess whether siRNA could be loaded into BLs prepared by each method, we used a fluorescence-activated cell sorter, the FACSCanto. As shown in Figure 2, BLs were successfully loaded with siRNA with both methods. The solution of chol-FITC-siRNA only could not be detected. Approximately 33% of the chol-si-BLs prepared by Method II were FITC positive. In contrast, the chol-si-BLs prepared by Method I were more heavily loaded with siRNA; approximately 80% were FITC positive. Thus, in all subsequent experiments, chol-si-BLs prepared by Method I were used. As shown in Table 1, there was almost no change in the size and zeta potential of the BLs after siRNA was added. We examined the change in the amount of siRNA bound to BLs when the concentration of siRNA was increased from 0.02 mol% to 0.4 mol% total lipids. As shown in Figure 3, the amount siRNA-loaded increased in a dose-dependent manner. We also investigated the stability of siRNA in the presence of RNase. The siRNA held by BLs showed increased stability in 0.1% RNase compared to free chol-siRNA, although some siRNA was degraded (Figure 4).

Co-transfection of pDNA and siRNA into cells using chol-si-BLs

To investigate the gene-silencing effects of siRNA transfection with chol-si-BLs and US, cells were co-transfected with pDNA encoding firefly luciferase (pCMV-GL3) and a random control or luciferase-targeting siRNA (siRandom or siLuc) in the concentration range of 0.02–0.4 mol% of total lipid (Figure 5A). Approximately 90% of luciferase expression was specifically blocked by siLuc of 0.1 mol% in the chol-si-BLs-treated group. We examined the effects of US exposure time on the downregulation of luciferase expression. As a result, transfection with chol-si-BLs and US exposure for only 5 s could deliver siRNA and pDNA into the cell; approximately 80% luciferase expression was specifically blocked (Figure 5B). The downregulation effects by siRNA were unaffected by the US exposure time, although luciferase expression was increased in

Table 1. Size (nm) and zeta potential (mV) of BLs and chol-si-BLs.

Lipid composition of BLs (molar ratio)	Mean size	zeta potential
BLs (DPPC: PEG2000 = 94:6)	519.2 ± 67.5 nm	−0.73 ± 0.12 mV
chol-si-BLs (DPPC:PEG2000: chol-siRNA = 94:6:0.1)	491.4 ± 55.9 nm	−0.47 ± 0.31 mV

DPPC, 1,2-dipalmitoyl-sn-glycero-phosphatidylcholine.

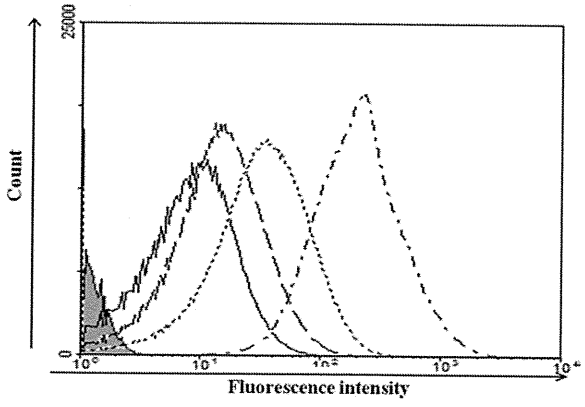

Figure 3. Loading of chol-siRNA into BLs. The interaction was examined by analyzing a solution of chol-si-BLs containing chol-FITC-siRNA (0.02–0.40 mol% of total lipid) with FACSCanto. Gray area: BLs only; solid line: chol-si-BLs (siRNA 0.02 mol%); dashed line: chol-si-BLs (siRNA 0.06 mol%); dotted line: chol-si-BLs (siRNA 0.10 mol%); dashed-dotted line: chol-si-BLs (siRNA 0.40 mol%).

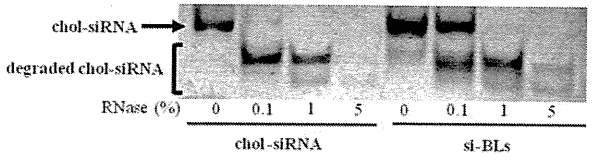

Figure 4. Stability of siRNA in the presence of RNase. Naked chol-siRNA or chol-si-BLs were subjected to 0–5% RNase degradation at 37°C for 30 min and confirmed by 20% acrylamide gel electrophoresis.

an US exposure time-dependent manner. Cytotoxicity was absent after US exposure within 10 s (Figure 5C). We also investigated the effects of US intensity ranging from 0.5 to 2.5 W/cm². The downregulation effects by siRNA were unaffected by the US intensity and cytotoxicity was absent after transfection (data not shown).

Transfection of siRNA using chol-si-BLs into stable cell lines

We performed siRNA transfection into Colon26-Luc to examine the effects of siRNA against endogenous gene expression. As shown in Figure 6A, there were no effects of specific gene-silencing; therefore, we attempted siRNA transfection into the cells in suspension. As a result, approximately 50% luciferase expression was specifically blocked by siLuc of 0.1 mol% in the chol-si-BLs-treated group (Figure 6B); however, the

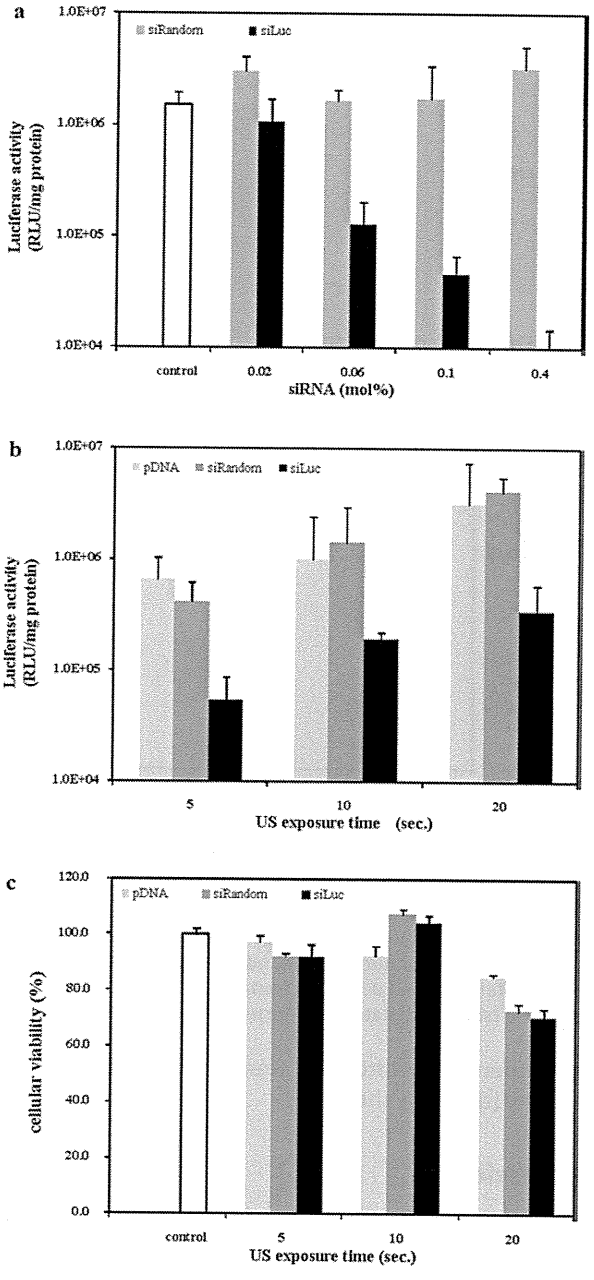

Figure 5. Downregulation of luciferase expression by siRNA. Luciferase expression in COS-7 cells transfected with pDNA and siRNA using chol-si-BLs and ultrasound (US) (frequency, 2 MHz; duty, 50%; burst rate, 2.0 Hz; intensity 2.5 W/cm²; time, 10 s) at 2-days post-transfection. (A) Effect of the amount of siRNA on gene-silencing effects. Control: group transfected with pCMV-GL3 only, siRandom: group transfected with pCMV-GL3 and non-targeting siRNA (siRandom), siLuc: group transfected with pCMV-GL3 and siRNA targeting luciferase (siLuc). (B) Effect of US exposure time on gene-silencing effects. (C) Effect of US exposure time on cellular viability. pDNA: group transfected with pCMV-GL3 only, siRandom: group transfected with pCMV-GL3 and non-targeting siRNA (siRandom), siLuc: group transfected with pCMV-GL3 and siRNA targeting luciferase (siLuc). All data are reported as the mean ± SD ($n = 4$).

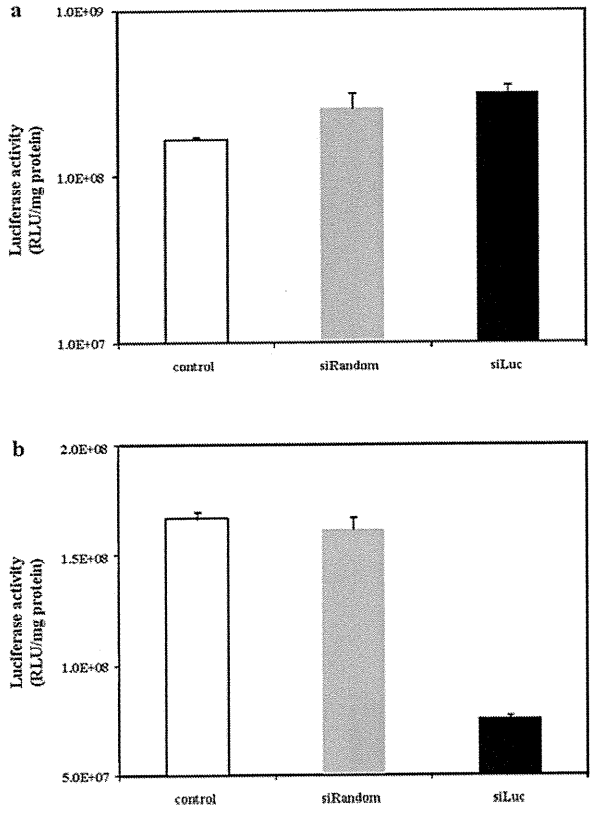

Figure 6. Downregulation of luciferase expression by siRNA. Luciferase expression in Colon26-Luc cells transfected with siRNA using chol-si-BLs and US at 2-days post-transfection. (A) Effect of chol-siRNA transfection into cells under adherent conditions. (B) Effect of chol-siRNA transfection into cells in suspension. Control: untreated group, siRandom: group transfected with non-targeting siRNA (siRandom), siLuc: group transfected with siRNA targeting luciferase (siLuc). All data are reported as the mean ± SD ($n=4$).

experimental conditions of transfection decreased cell viability (data not shown).

Discussion

The specific silencing of gene expression through RNAi has great potential to address previously untreatable diseases. The safe and effective delivery of siRNA, however, remains challenging. We have developed BLs and shown that they were an effective and novel tool for gene and siRNA delivery *in vitro* and *in vivo* (Suzuki et al., 2007, 2008a,b; Negishi et al., 2008). The siRNA transfection by the combination of BLs and US exposure delivers siRNA into only US-exposed area after systemic injection; however, our previous data were obtained using a mixture of BLs and naked siRNA. Therefore, BLs and siRNA did not colocalize in blood vessels after intravenous administration. Additionally, siRNA is susceptible to rapid removal from the circulation and degradation by nucleases, leading to a reduction in transfection efficiency *in vivo*. In this study, we prepared chol-si-BLs-containing chol-siRNA as a more effective, efficient delivery tool for systemic injections. Cholesterol is often used for the preparation of liposomes, and thus chol-siRNA seems to embed easily in the lipid bilayer.

We initially investigated the optimal method for preparation of chol-si-BLs, and then used flow cytometry to examine the interaction between siRNA and BLs. The BLs were detectable, although the fluorescence intensity was low. Fluorescein-labeled siRNA molecules were too small to be detected with flow cytometry; however, the chol-si-BLs exhibited strong fluorescence. We compared Method I (adding chol-siRNA to the lipid mixture and preparing liposomes by REV method) with Method II (simply mixing BLs and chol-siRNA). As shown in Figure 2, BLs could be loaded with much more chol-siRNA by Method I, although chol-siRNA could interact with BLs both methods were used. These results suggested that chol-siRNA of chol-si-BLs by Method I might not only be embedded in the lipid layer but also encapsulated in the liposomes. Additionally, we examined the change in the amount of bound chol-siRNA by adding various amounts of chol-siRNA to the lipid mixture. As shown in Figure 3, the amount of chol-siRNA loaded into BLs increased with chol-siRNA addition in a dose-dependent manner for up to 0.4 mol% of the total lipid content. We also investigated the stability of siRNA interacting with BLs in RNase. Although some siRNA was degraded, siRNA held by BLs showed increased stability in 0.1% RNase compared to free chol-siRNA (Figure 4). The chol-siRNA embedded in the outside lipid layer of BLs seemed susceptible to degradation by nucleases. It has been reported that the modification of liposomes with short and long PEG chains increases the fixed aqueous layer thickness (Sadzuka et al., 2002). In this study, we prepared BLs with only one type of PEG chain length; therefore, BLs with short and long PEG might improve the stability of siRNA. In Figure 4, the electrophoresis data also indicated that there was no damage to chol-siRNA from sonication for the preparation of chol-si-BLs. The fact was also supported by the gene-silencing effects by chol-siRNA in Figure 5 and 6.

We examine the gene-silencing effects of chol-siRNA transfected chol-si-BLs and US. The expression of luciferase in cells was efficiently inhibited in a siLuc dose-dependent manner (Figure 5A). The concentration range of 0.02–0.4 mol% of the total lipid, was equivalent to 25–500 nM. Approximately 80% luciferase expression was specifically blocked by siLuc of more than 0.06 mol%. The condition of US exposure affects the efficiency of US-mediated gene transfection (Duvshani-Eshet and Machluf, 2005; Mitragotri, 2005); therefore, we also investigated the effects of US exposure time on the downregulation of luciferase expression (Figure 5B and 5C). As a result, approximately 80% luciferase expression was specifically blocked and cytotoxicity was absent after transfection within 10 s. The downregulation effects by siRNA were unaffected by intensity of the US; thus, showing that the US condition (frequency, 2 MHz; duty, 50%; burst rate, 2.0 Hz; intensity, 2.5 W/cm^2; time,

10 s) were appropriate for siRNA transfection by chol-si-BLs. These results correlate with our previous study (Negishi et al., 2008). Interestingly, the downregulation effects by siRNA were unaffected by the US exposure time, although luciferase expression was increased in an US exposure time-dependent manner. There are two possible reasons for this result. First, the size of molecule may effect on the transport of molecules via transient pores by cavitation. Second, the US exposure time may effect on the transport amount of pDNA to the nucleus. Plasmid DNA needs to enter the nucleus for effective therapy. On the other hand, siRNA is known to function in the cytosol. The detailed mechanism of this transfection method remains unknown and should be studied in the future. It was also pointed out that the exposure to US induced cavitation, the release of siRNA from chol-si-BLs, and the delivery of siRNA into the cytoplasm within a fairly short time; however, it is necessary to perform the experiment with siRNA targeting endogenous genes considering the application of synthetic siRNA to the treatment of disease. We then attempted siRNA transfection into the cells stably expressing firefly luciferase, Colon26-Luc cells. There were no effects of specific gene-silencing by siRNA transfection under the same conditions used so far (Figure 6A). This result suggested that the amount of siRNA transfected into cells was insufficient for the downregulation of endogenous gene expression. We therefore changed the transfection conditions using cells in suspension, not in an adherent condition. As shown in Figure 6B, approximately 50% luciferase expression was specifically blocked, although cell viability was decreased. These data demonstrated that the suspended cells were more likely to be affected by US energy than adherent cells and the amount of siRNA transfected into cells was increased. It is expected that the combination of chol-si-BLs and US exposure will be a safe and an effective siRNA transfection system after a more detailed examination of the US conditions. Cholesterol is one of the major components of the eukaryotic cell membrane, and is highly distributed in plasma membranes (Lange et al., 1989). Cholesterol fits its non-polar part between alkyl chains of phospholipids, and is appropriate for incorporation into the phospholipid bilayer due to its easy-to-fit structure and its physical influence on membrane properties such as fluidity and permeability. Thus, cholesterol is often used to prepare liposomes as not only membrane models but also drug carriers. BLs stability was considered to be unaffected by the cholesterol content in this study (0.02–0.4 mol% of total lipid). Indeed, liposomes containing chol-siRNA entrapped the gas and could be used as US contrast agents as well as conventional BLs without cholesterol (data not shown). In addition, chol-siRNA might not be easy to release from the lipid bilayer, although it seemed to embed easily. The amount of chol-siRNA transfected into cells would be efficiently increased if its release rate from lipid by US exposure could be increased. In the future, we will examine siRNA delivery via systemic injection and its own disease-associated gene-silencing effects. It was reported that chol-siRNA could improve pharmacokinetic and cellular uptake in mice via systemic injection (Soutschek et al., 2004). The mechanisms of improved distribution and cellular uptake of siRNA through cholesterol conjugation were also demonstrated in a recent study; chol-siRNA seemed to be incorporate into circulating lipoprotein particles and was efficiently internalized via receptor-mediated processes (Wolfrum et al., 2007). Therefore, chol-siRNA alone tends to be delivered to limited tissues such as the liver, adrenal, and kidney; however, the chol-si-BLs developed in this study enabled site-specific siRNA delivery to other tissues in combination with transdermal US exposure. Additionally, microbubbles modified with an antibody and having a targeting function have recently been developed (Leong-Poi et al., 2005; Behm et al., 2008; Palmowski et al., 2008). Liposomes can be easily modified to add a targeting function; thus, chol-si-BLs using an antibody or peptide will enable more efficient siRNA delivery only to target cells in combination with US exposure and lead to beneficial clinical applications for various diseases.

Conclusion

In this study, we showed that BLs could efficiently load chol-siRNA and protect siRNA against nuclease degradation. Additionally, chol-si-BLs could deliver siRNA to cells, although there remains room for improvement. These results suggest that chol-si-BLs with US exposure may be useful for delivering siRNA to a tissue or organ via systemic injection.

Acknowledgements

The authors are grateful to Prof. Katsuro Tachibana (Department of Anatomy, School of Medicine, Fukuoka University) for technical advice regarding the induction of cavitation with US, and to Mr. Yasuhiko Hayakawa and Mr. Kosho Suzuki (NEPA GENE Co., Ltd.) for technical advice regarding US exposure.

Declaration of interest

This study was supported by a Grant for Industrial Technology Research (04A05010) from the New Energy and Industrial Technology Development Organization (NEDO) of Japan, a Grant-in-aid for Scientific Research (B) (20300179) from the Japan Society for the Promotion of Science, a Grant-in-aid for Scientific Research (B) (19300185) from the Japan Society for the Promotion of Science, and a Grant-in-aid for Young Scientists (B) (21790164) from the Japan Society for the Promotion of Science. Kazuo Maruyama acknowledges the Program for Promotion of Fundamental Studies (Project ID: 10–23) in Health Sciences of the National Institute of Biomedical Innovation (NIBIO).

References

Allen TM, Hansen C, Martin F, Redemann C, Yau-Young A. (1991). Liposomes containing synthetic lipid derivatives of poly(ethylene glycol) show prolonged circulation half-lives *in vivo*. Biochim Biophys Acta, 1066, 29-36.

Behm CZ, Kaufmann BA, Carr C, Lankford M, Sanders JM, Rose CE, Kaul S, Lindner JR. (2008). Molecular imaging of endothelial vascular cell adhesion molecule-1 expression and inflammatory cell recruitment during vasculogenesis and ischemia-mediated arteriogenesis. Circulation, 117, 2902-2911.

Blume G, Cevc G. (1990). Liposomes for the sustained drug release *in vivo*. Biochim Biophys Acta, 1029, 91-97.

Duvshani-Eshet M, Machluf M. (2005). Therapeutic ultrasound optimization for gene delivery: A key factor achieving nuclear DNA localization. J Control Release, 108, 513-528.

Harata M, Soda Y, Tani K, Ooi J, Takizawa T, Chen M, Bai Y, Izawa K, Kobayashi S, Tomonari A, Nagamura F, Takahashi S, Uchimaru K, Iseki T, Tsuji T, Takahashi TA, Sugita K, Nakazawa S, Tojo A, Maruyama K, Asano S. (2004). CD19-targeting liposomes containing imatinib efficiently kill Philadelphia chromosome-positive acute lymphoblastic leukemia cells. Blood, 104, 1442-1449.

Kinoshita M, Hynynen K. (2005). A novel method for the intracellular delivery of siRNA using microbubble-enhanced focused ultrasound. Biochem Biophys Res Commun, 335, 393-399.

Lange Y, Swaisgood MH, Ramos BV, Steck TL. (1989). Plasma membranes contain half the phospholipid and 90% of the cholesterol and sphingomyelin in cultured human fibroblasts. J Biol Chem, 264, 3786-3793.

Leong-Poi H, Christiansen J, Heppner P, Lewis CW, Klibanov AL, Kaul S, Lindner JR. (2005). Assessment of endogenous and therapeutic arteriogenesis by contrast ultrasound molecular imaging of integrin expression. Circulation, 111, 3248-3254.

Li T, Tachibana K, Kuroki M, Kuroki M. (2003). Gene transfer with echo-enhanced contrast agents: Comparison between Albunex, Optison, and Levovist in mice-initial results. Radiology, 229, 423-428.

Maruyama K, Ishida O, Kasaoka S, Takizawa T, Utoguchi N, Shinohara A, Chiba M, Kobayashi H, Eriguchi M, Yanagie H. (2004). Intracellular targeting of sodium mercaptoundecahydrododecaborate (BSH) to solid tumors by transferrin-PEG liposomes, for boron neutron-capture therapy (BNCT). J Control Release, 98, 195-207.

Maruyama K, Yuda T, Okamoto A, Kojima S, Suginaka A, Iwatsuru M. (1992). Prolonged circulation time *in vivo* of large unilamellar liposomes composed of distearoyl phosphatidylcholine and cholesterol containing amphipathic poly(ethylene glycol). Biochim Biophys Acta, 1128, 44-49.

Mitragotri S. (2005). Healing sound: The use of ultrasound in drug delivery and other therapeutic applications. Nat Rev Drug Discov, 4, 255-260.

Negishi Y, Endo Y, Fukuyama T, Suzuki R, Takizawa T, Omata D, Maruyama K, Aramaki Y. (2008). Delivery of siRNA into the cytoplasm by liposomal bubbles and ultrasound. J Control Release, 132, 124-130.

Palmowski M, Huppert J, Ladewig G, Hauff P, Reinhardt M, Mueller MM, Woenne EC, Jenne JW, Maurer M, Kauffmann GW, Semmler W, Kiessling F. (2008). Molecular profiling of angiogenesis with targeted ultrasound imaging: Early assessment of antiangiogenic therapy effects. Mol Cancer Ther, 7, 101-109.

Sadzuka Y, Nakade A, Hirama R, Miyagishima A, Nozawa Y, Hirota S, Sonobe T. (2002). Effects of mixed polyethyleneglycol modification on fixed aqueous layer thickness and antitumor activity of doxorubicin containing liposome. Int J Pharm, 238, 171-180.

Sonoda S, Tachibana K, Uchino E, Okubo A, Yamamoto M, Sakoda K, Hisatomi T, Sonoda KH, Negishi Y, Izumi Y, Takao S, Sakamoto T. (2006). Gene transfer to corneal epithelium and keratocytes mediated by ultrasound with microbubbles. Invest Ophthalmol Vis Sci, 47, 558-564.

Soutschek J, Akinc A, Bramlage B, Charisse K, Constien R, Donoghue M, Elbashir S, Geick A, Hadwiger P, Harborth J, John M, Kesavan V, Lavine G, Pandey RK, Racie T, Rajeev KG, Röhl I, Toudjarska I, Wang G, Wuschko S, Bumcrot D, Koteliansky V, Limmer S, Manoharan M, Vornlocher HP. (2004). Therapeutic silencing of an endogenous gene by systemic administration of modified siRNAs. Nature, 432, 173-178.

Suzuki R, Takizawa T, Negishi Y, Hagisawa K, Tanaka K, Sawamura K, Utoguchi N, Nishioka T, Maruyama K. (2007). Gene delivery by combination of novel liposomal bubbles with perfluoropropane and ultrasound. J Control Release, 117, 130-136.

Suzuki R, Takizawa T, Negishi Y, Utoguchi N, Maruyama K. (2008a). Effective gene delivery with novel liposomal bubbles and ultrasonic destruction technology. Int J Pharm, 354, 49-55.

Suzuki R, Takizawa T, Negishi Y, Utoguchi N, Sawamura K, Tanaka K, Namai E, Oda Y, Matsumura Y, Maruyama K. (2008b). Tumor specific ultrasound enhanced gene transfer *in vivo* with novel liposomal bubbles. J Control Release, 125, 137-144.

Taniyama Y, Tachibana K, Hiraoka K, Aoki M, Yamamoto S, Matsumoto K, Nakamura T, Ogihara T, Kaneda Y, Morishita R. (2002a). Development of safe and efficient novel nonviral gene transfer using ultrasound: Enhancement of transfection efficiency of naked plasmid DNA in skeletal muscle. Gene Ther, 9, 372-380.

Taniyama Y, Tachibana K, Hiraoka K, Namba T, Yamasaki K, Hashiya N, Aoki M, Ogihara T, Yasufumi K, Morishita R. (2002b). Local delivery of plasmid DNA into rat carotid artery using ultrasound. Circulation, 105, 1233-1239.

Tsunoda S, Mazda O, Oda Y, Iida Y, Akabame S, Kishida T, Shin-Ya M, Asada H, Gojo S, Imanishi J, Matsubara H, Yoshikawa T. (2005). Sonoporation using microbubble BR14 promotes pDNA/siRNA transduction to murine heart. Biochem Biophys Res Commun, 336, 118-127.

Unger EC, Porter T, Culp W, Labell R, Matsunaga T, Zutshi R. (2004). Therapeutic applications of lipid-coated microbubbles. Adv Drug Deliv Rev, 56, 1291-1314.

Wolfrum C, Shi S, Jayaprakash KN, Jayaraman M, Wang G, Pandey RK, Rajeev KG, Nakayama T, Charrise K, Ndungo EM, Zimmermann T, Koteliansky V, Manoharan M, Stoffel M. (2007). Mechanisms and optimization of *in vivo* delivery of lipophilic siRNAs. Nat Biotechnol, 25, 1149-1157.

Biomaterials 32 (2011) 162–169

Contents lists available at ScienceDirect

Biomaterials

journal homepage: www.elsevier.com/locate/biomaterials

Development of an antibody proteomics system using a phage antibody library for efficient screening of biomarker proteins

Sunao Imai [a,1], Kazuya Nagano [a,1], Yasunobu Yoshida [a], Takayuki Okamura [a], Takuya Yamashita [a,b], Yasuhiro Abe [a], Tomoaki Yoshikawa [a,b], Yasuo Yoshioka [a,b,c], Haruhiko Kamada [a,c], Yohei Mukai [a,b], Shinsaku Nakagawa [b,c], Yasuo Tsutsumi [a,b,c], Shin-ichi Tsunoda [a,b,c,*]

[a] Laboratory of Biopharmaceutical Research, National Institute of Biomedical Innovation, 7-6-8 Saito-Asagi, Ibaraki, Osaka 567-0085, Japan
[b] Graduate School of Pharmaceutical Sciences, Osaka University, 1-6 Yamadaoka, Suita, Osaka 565-0871, Japan
[c] The Center of Advanced Medical Engineering and informatics, Osaka University, 1-6 Yamadaoka, Suita, Osaka 565-0871, Japan

ARTICLE INFO

Article history:
Received 27 August 2010
Accepted 14 September 2010
Available online 8 October 2010

Keywords:
Protein
Image analysis
Immunochemistry
Molecular biology
Antibody
Cancer

ABSTRACT

Proteomics-based analysis is currently the most promising approach for identifying biomarker proteins for use in drug development. However, many candidate biomarker proteins that are over- or under-expressed in diseased tissues are found by such a procedure. Thus, establishment of an efficient method for screening and validating the more valuable targets is urgently required. Here, we describe the development of an "antibody proteomics system" that facilitates the screening of biomarker proteins from many candidates by rapid preparation of cross-reacting antibodies using phage antibody library technology. Using two-dimensional differential in-gel electrophoresis analysis, 16 over-expressed proteins from breast cancer cells were identified. Specifically, proteins were recovered from the gel pieces and a portion of each sample was used for mass spectrometry analysis. The remainder was immobilized onto a nitrocellulose membrane for antibody-expressing phage enrichment and selection. Using this procedure, antibody-expressing phages against each protein were successfully isolated within two weeks. The expression profiles of the identified proteins were then acquired by immunostaining of breast tumor tissue microarrays with the antibody-expressing phages. Using this approach, expression of Eph receptor A10, TRAIL-R2 and Cytokeratin 8 in breast tumor tissues were successfully validated.

These results demonstrate the antibody proteomics system is an efficient method for screening tumor-related biomarker proteins.

1. Introduction

Proteomics-based analysis is the most promising approach for identifying tumor-related biomarker proteins used in the drug development process [1–3]. The technological development of proteomics to seek and identify differentially expressed proteins in disease samples is expanding rapidly. However, in spite of the identification of many candidate biomarkers, the number of biomarker proteins successfully applied to drug development has been limited. The main difficulty is the lack of a methodology to comprehensively analyze the expression or function of many candidate proteins and to efficiently select potential biomarker proteins of interest. To circumvent this problem, an improved technology to efficiently screen the truly valuable proteins from a large number of candidates is desirable.

Monoclonal antibodies are extremely useful tools for the functional and distributional analysis of proteins [4–6]. For example, they can be applied to the specific detection and study of proteins through various techniques including ELISA, Western blotting, fluorescent imaging and tissue microarray analysis (TMA). Of all these techniques, TMA is particularly valuable because it enables the analysis of clinical expression profiles of antigens from many clinical samples [7–11]. However, the common hybridoma-based antibody production is a laborious and time-consuming method. Thus, it is impractical to create antibodies against many differentially expressed proteins identified by proteomics technologies, such as two-dimensional differential in-gel electrophoresis (2D-DIGE) [12–15]. Furthermore, a relatively large amount of antigen (several milligrams) is necessary to produce an antibody (i.e., immunization of animals or screening of positive clones). The

* Corresponding author. Laboratory of Biopharmaceutical Research, National Institute of Biomedical Innovation, 7-6-8 Saito-Asagi, Ibaraki, Osaka 567-0085, Japan. Tel.: +81 72 641 9814; fax: +81 72 641 9817.
E-mail address: tsunoda@nibio.go.jp (S.-i. Tsunoda).
[1] These authors contributed equally to the work.

0142-9612/$ – see front matter © 2010 Elsevier Ltd. All rights reserved.
doi:10.1016/j.biomaterials.2010.09.030

production of protein on this scale often requires engineering the corresponding gene for heterologous expression, which may require some time to optimize. In this respect, phage antibody library technology is able to construct a large repertoire protein or peptide consisting of hundreds of millions of molecules. Monoclonal antibodies against target antigens are then rapidly obtained from the phage libraries displaying single chain fragment variable (scFv) antibodies *in vitro* [16–21].

However, the amount of protein in spots detected by 2D-DIGE analysis is generally very small (hundreds of nanograms). Therefore, a technology for generating monoclonal antibodies from such small amounts of antigen needs to be developed. There are no reports that describe the successful isolation of antibodies against small amounts of proteins obtained from differential proteome analysis.

Here, we report the establishment of a method for the efficient isolation of scFv antibody-expressing phages from a small amount of protein antigen prepared *via* 2D-DIGE spots using a high quality non-immune mouse scFv phage library [22]. We also describe an efficient method for screening and validating tumor-related biomarker proteins of interest from a number of differentially expressed proteins by expression profiling using TMA and scFv antibody-expressing phages.

2. Materials and methods

2.1. Non-immune mouse scFv phage library

Construction of the improved non-immune murine scFv phage library has been described previously [22]. The phage library was prepared from a TG1 glycerol stock containing the scFv gene library.

2.2. Affinity panning using BIAcore® and nitrocellulose membrane

Three different amounts (5000 ng, 50 ng or 0.5 ng) of KDR-Fc chimera (R&D systems Inc., Minneapolis, MN) or a portion of the proteins (1–5 ng) extracted from 2D-DIGE spots were immobilized on a BIAcore sensor chip CM3® (BIAcore, Uppsala, Sweden) or on a nitrocellulose membrane. BIAcore-based panning has been described previously [22]. Membrane-based panning was performed using the Bio-Dot Microfiltration Apparatus (Bio-Rad Laboratories, Hercules, CA). The membrane was incubated with blocking solution (10% skimmed milk, 25% glycerol) for 2 h and then washed twice with 0.1% TBST (Tris-buffered saline containing 0.1% Tween 20). The model phage library (anti-KDR scFv antibody-expressing phages: wild type phage = 1: 100) or the non-immune scFv phage library was pre-incubated with 90% blocking solution at 4 °C for 1 h and then applied to each well. After 2–3 h incubation, the apparatus was washed ten times with TBST. Bound scFv antibody-expressing phages were then eluted with 100 mM triethylamine. The eluted phages were incubated in log phase *E. coli* TG1 cells and glycerol-stocks prepared for further repeat panning cycles. Phage titer was measured by counting the number of infected colony cells on Petrifilm (3M Co., St. Paul, MN).

2.3. Colony direct PCR

After the panning, colonies of phage-infected TG1 were picked up at random as PCR templates. The gene inserts of 16 clones were amplified by PCR using the following primers: primer-156 (5′-CAACGTGAAAAAATTATTATTCGC-3′) and primer-158 (5′-GTAAATGA ATTTTCTGTATGAGG-3′), which anneal to the sequences of pCANTAB5E phagemid vector (GE Healthcare Biosciences AB, Uppsala, Sweden). The size of insert DNA sequence was analyzed by agarose gel electrophoresis.

2.4. Cell lines

Human mammary gland cell line 184A1 (American Type Culture Collection; ATCC, Manassas, VA) was maintained by MEGM Bullet Kit (Takara Bio, Shiga, JAPAN). Mammary gland-derived breast cancer cell line SKBR3 (ATCC) was maintained in McCoy's 5a plus 10% FBS. All cells were grown at 37 °C in a humidified incubator with 5% CO_2.

2.5. 2D-DIGE analysis

Cell lysates were prepared from human mammary gland cell line 184A1 and mammary gland-derived breast cancer cell line SKBR3, and then solubilized with 7 M urea, 2 M thiourea, 4% CHAPS and 10 mM Tris–HCl (pH 8.5). The lysates were labeled at the ratio 50 μg protein: 400 pmol Cy3 or Cy5 protein labeling dye (GE Healthcare Biosciences AB) in dimethylformamide according to the manufacture's protocol. For first dimension separation, the labeled samples (each 50 μg) were combined and mixed with rehydration buffer (7 M urea, 2 M thiourea, 4% CHAPS, 2% DTT, 2% Pharmalyte (GE Healthcare Biosciences AB)) and applied to a 24-cm immobilized pH gradient gel strip (IPG-strip pH 5–6 NL). The samples for the spot-picking gel were prepared without labelling by Cy-dyes. For the second dimension separation, the IPG-strips were applied to SDS-PAGE gels (10% polyacrylamide and 2.7% N,N′-diallyltartardiamide gels). After electrophoresis, the gels were scanned with a laser fluoroimager (Typhoon Trio, GE Healthcare Biosciences AB). The spot-picking gel was scanned after staining with Flamingo solution (Bio-Rad). Quantitative analysis of protein spots was carried out with Decyder-DIA software (GE Healthcare Biosciences AB). For the antigen spots of interest, spots of 1 × 1 mm in size were picked using an Ettan Spot Picker (GE Healthcare Biosciences AB). Proteins were extracted by solubilizing the picked gel pieces using 88 mM sodium periodide. Protein volumes were determined by BSA standard in Colloid Gold Total Protein staining (Bio-Rad).

2.6. In-gel tryptic digestion

Spots of 1 mm × 1 mm in size were picked using an Ettan Spot Picker and digested with trypsin as described below. The gel pieces were then destained with 50% acetonitrile/50 mM NH_4HCO_3 for 20 min twice, dehydrated with 75% acetonitrile for 20 min, and then dried using a centrifugal concentrator. Next, 5 μl of 20 μl/ml trypsin (Promega, Madison, WI) solution was added to each gel piece and incubated for 16 h at 37 °C. Three solutions were used to extract the resulting peptide mixtures from the gel pieces. First, 50 μl of 50% (v/v) acetonitrile in 1% (v/v) aqueous trifluoroacetic acid (TFA) was added to the gel pieces, which were then sonicated for 5 min. Next, we collected the solution and added 80% (v/v) acetonitrile in 0.2% TFA. Finally, 100% acetonitrile was added for the last extraction. The peptides were dried and then resuspended in 10 μl of 0.1% TFA before being cleaned using ZipTip™ μC_{18} pipette tips (Millipore, Billerica, MA). The tips were wetted with three washes in 50% acetonitrile and equilibrated with three washes in 0.1% TFA, then the peptides were aspirated 10 times to ensure binding to the column. The column and peptides were washed three times in 0.1% TFA before being eluted in 1 μl of 80% acetonitrile/0.2% TFA.

2.7. Mass spectrometry (MS) and database search

The tryptic digests (0.6 μl) were mixed with 0.6 μl α-cyano-4-hydroxy-trans-cinnamic acid saturated in a 0.1% TFA and acetonitrile solution (1:1vol/vol). Each mixture was deposited onto a well of a 96-well target plate and then analyzed by matrix-assisted laser desorption ionization time-of-flight mass spectrometry (MALDI-TOF/MS; autoflexII, Bruker Daltonics, Billerica, WI) in the Reflectron mode. The mass axis was adjusted with calibration peptide (BRUKER DALTNICS) peaks (M/z 1047.19, 1296.68, or 2465.19) as lock masses. Bioinformatic databases were searched to identify the proteins based on the tryptic fragment sizes. The Mascot search engine (http://www.matrixscience.com) was initially used to query the entire theoretical tryptic peptide as well as SwissProt (http://www.expasy.org/, a public domain database provided by the Swiss Institute of Bioinformatics, Geneva, Switzerland). The search query assumed the following: (i) the peptides were monoisotopic (ii) methionine residues may be oxidized (iii) all cysteines are modified with iodoacetamide.

2.8. Phage ELISA using nitrocellulose membrane

Phage ELISA using scFv antibody-expressing phages was performed as previously described [22]. Briefly, phage-infected TG1 clones were picked, monocloned in a Bio-Dot Microfiltration Apparatus and scFv antibody-expressing phages propagated. The supernatants containing scFv antibody-expressing phages were incubated with immobilized proteins (~1 ng) extracted from 2D-DIGE spots. scFv antibody-expressing phages bound to 2D-DIGE spots were visualized using HRP-conjugated anti-M13 monoclonal antibody (GE Healthcare Biosciences AB).

2.9. Immunohistochemical staining using scFv antibody-expressing phages

Human breast cancer and normal TMA (Super Bio Chips, Seoul, South Korea & Biomax, Rockville, MD) were deparaffinated in xylene and rehydrated in a graded series of ethanol. Heat-induced epitope retrieval was performed in while keeping Target Retrieval Solution pH 9 (Dako, Glostrup, Denmark) temperature following the manufacturer's instructions. Heat-induced epitope retrieval was performed while maintaining the Target Retrieval Solution pH 9 (Dako) at the desired temperature according to the manufacturer's instructions. After heat-induced epitope retrieval treatment, endogenous peroxidase was blocked with 0.3% H_2O_2 in TBS for 5 min followed by washing twice in TBS. TMA were incubated with 5% BSA blocking solution for 15 min. The slides were then incubated with the primary scFv antibody-expressing phages (10^{12} CFU/ml) for 60 min. After washing three times with 0.05% TBST, each series of sections was incubated for 30 min with ENVISION + Dual Link (Dako), washed three times in TBST. The reaction products were rinsed twice with TBST, and then developed in liquid 3,3′-diaminobenzidine (Dako) for 3 min. After the development, sections were washed twice with distilled water, lightly

counterstained with Mayer's hematoxylin, dehydrated, cleared, and mounted with resinous mounting medium. All procedures were performed using AutoStainer (Dako).

2.10. TMA Immunohistochemistry scoring

The optimized staining condition for breast tumor tissue microarray was determined based on the coexistence of both positive and negative cells in the same tissue sample. Signals were considered positive when reaction products were localized in the expected cellular component. The criteria for the staining were scored as follows: distribution score was scored as 0 (0%), 1 (1–50%), and 2 (51–100%) to indicate the percentage of positive cells in all tumor cells present in one tissue. The intensity of the signal (intensity score) was scored as 0 (no signal), 1 (weak), 2 (moderate) or 3 (marked). The total of the distribution score and intensity score was then summed into a total score (TS) of TS0 (sum = 0), TS1 (sum = 2), TS2 (sum = 3), and TS3 (sum = 4–5). Throughout this study, TS0 or TS1 was regarded as negative, whereas TS2 or TS3 was regarded as positive. Statview software was used in statistical analysis.

3. Results

3.1. Optimization of panning methods

To establish a method for the efficient isolation of antibodies against a small amount of protein antigen (nanogram-order or less) prepared from 2D-DIGE spots, 5000 ng, 50 ng or 0.5 ng of recombinant KDR proteins were first immobilized on a BIAcore sensor chip CM3® or on a nitrocellulose membrane using the Bio-Dot Microfiltration Apparatus®. Isolation of antibodies was assessed using a model phage library (anti-KDR scFv antibody-expressing phages: wild type phage = 1: 100) (Fig. 1). Enrichment of the desired clones in the output library was evaluated by analyzing the gene inserts of randomly-picked phage-infected TG1 cells by colony direct PCR. In the method using BIAcore®, enrichment was observed when 5000 ng of KDR was used for immobilization. By contrast, Membrane-based panning led to the successful enrichment of anti-KDR scFv antibodies from only 0.5 ng of KDR. These results demonstrated that membrane-based panning was suitable for the isolation of antibodies from very small amounts of antigen extracted from 2D-DIGE spot gel pieces.

3.2. 2D-DIGE analysis and identification of differentially expressed proteins

To identify breast tumor-related biomarker proteins and isolate monoclonal antibodies against them, we performed 2D-DIGE using breast cancer cell lines SKBR3 and normal breast cell lines 184A1 (Fig. 2). Quantitative analysis showed that 21 spots displayed increased or decreased expression levels in the cancer cell line compared with the normal cell line. MALDI-TOF/MS analysis of the spots subsequently identified 16 different proteins (Table 1).

3.3. Isolation of antibodies against each 2D-DIGE spot from the non-immune scFv phage library

The amount of protein extracted from the gel pieces ranged from several tens of nanogram to a few micrograms (Table 1). Because the membrane-based panning method facilitates the isolation of antibodies from 0.5 ng of protein (Fig. 1), we reasoned that this method could be used to isolate antibodies from the small amounts of proteins extracted from 2D-DIGE spot gel pieces. Thus a portion of the extracted proteins were immobilized onto nitrocellulose membranes by means of a Bio-Dot Microfiltration Apparatus, and membrane-based panning was performed using the non-immune scFv phage library [22] (Table 2). The results from this panning showed that the output/input ratio of phage titer (titer of the recovered phage library after the panning/titer of phage library before the panning) after the fourth round of panning against all spots increased approximately 20-fold–4000-fold in comparison to that obtained from the first round of panning. This elevated output/input ratio indicated the enrichment of the antigen-binding scFv antibody clones. To isolate monoclonal scFv antibodies to each spot, a total of 60 clones were randomly picked from the 4th panning output phage library and binding of the monoclonal scFv antibody-expressing phages to each antigen was tested by phage ELISA. As a result, several scFv antibody clones binding to each of the 16 antigens were isolated (Table 2). The antigenic specificity of isolated scFv antibodies was investigated by dot blot using various proteins as antigens. Some of the isolated scFv antibodies bound specifically to the antigen protein, but not to the His-tagged caspase-8, His-tagged importin-β, tumor necrosis factor receptor 1 (TNFR1)-Fc-chimera and KDR-Fc-chimera (data not shown). These results indicated the successful isolation of each spot-specific scFv antibody-expressing phages after only two weeks.

3.4. TMA analysis

The next stage in the process was to select the most valuable breast tumor-related biomarker proteins from a large number of

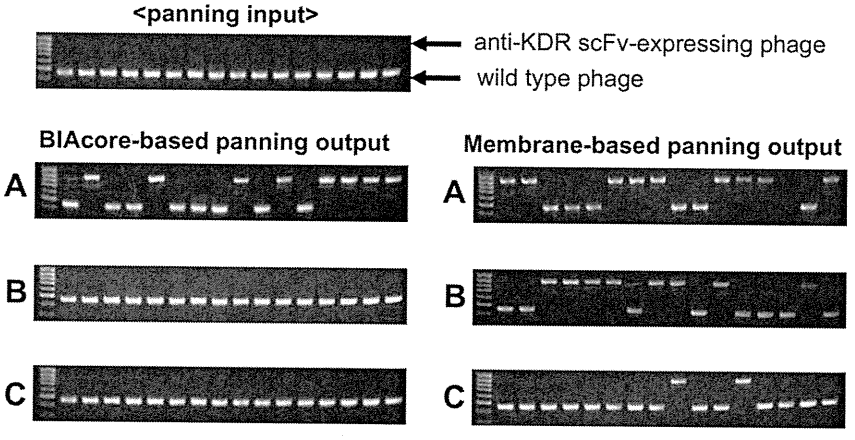

Fig. 1. Optimization of panning methods to isolate monoclonal antibodies from a very small amount of antigen. Model panning was performed using the BIAcore® or nitrocellulose membrane. The model library (anti-KDR scFv phage : wild type phage = 1: 100) was incubated with KDR ((A) 5000 ng, (B) 50 ng, (C) 0.5 ng) immobilized on a sensor chip or nitrocellulose membrane. The BIAcore-based panning method has been previously described [22]. After the binding step, the nitrocellulose membrane was washed ten times with TBST. The bound scFv antibody-expressing phages were eluted with triethylamine. The eluted scFv antibody-expressing phages were then incubated in log phase TG1 cells and individual TG1 clones were picked at random. Inserts of 16 phage clones were amplified by PCR. The gene sizes of inserts were analyzed by agarose gel electrophoresis.

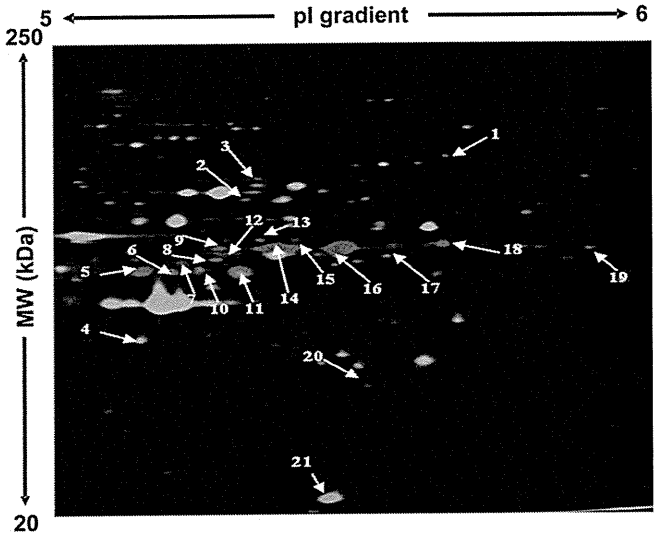

Fig. 2. 2D-DIGE image of fluorescently labeled proteins from SKBR3 and 184A cell. Breast cancer cell line (SKBR3) and normal breast cell line (184A1) were labeled using cy3 and cy5, respectively. The protein samples were then subjected to 2D electrophoresis. Spots that were over- and under-expressed in mammary cancer cells relative to normal cells were colored red and green, respectively. Yellow color spots show no change in expression.

identified candidate proteins. To this end, we immunostained TMA slides with 189 cases of breast tumors and 15 cases of normal breast specimens using the isolated spot-specific scFv antibody-expressing phages and screened the promising candidate biomarker proteins in terms of the expression profile in breast tumor tissues and normal tissues (Table 3). The result of the expression profile analysis showed that SPATA5, beta-actin variant, FLJ31438, PAK65, XRN1 and Jerky protein homolog-like were not expressed in normal and breast cancer tissue at all. By contrast, TRAIL-R2, Cytokeratin 8 and Eph receptor A10 were highly and specifically expressed (Fig. 3) in 63, 73 and 49% of breast tumor cases respectively, while the existing-breast cancer marker, Her-2, was expressed in 28% of breast tumor cases (Table 3). Thus, the relationship between the expression of each antigen and the Her-2 expression profile was analyzed. The level of expression of TRAIL-R2, Cytokeratin 8 and Eph receptor A10 in Her-2 positive cases were 77, 77 and 62%, and in Her-2 negative cases were 57, 67 and 44%, respectively (Table 4). Furthermore, the relationship between the expression of each antigen and clinical stage was analyzed in 187 of the 189 cases where all the clinical data was available. The level of expression of Cytokeratin 8 and Eph receptor A10 increased with progression of clinical symptoms (Table 5).

Table 1
Identification of 2D-DIGE spots by MALDI-TOF/MS.

Spot	Protein name	Accession number	MW (kDa)	pI	Protein volume (ng)	Expression ratio [cancer/normal] (fold)
#1	splicing factor YT521-B	Q96MU7	85	5.9	119	6
#2	IkappaBR	Q96HA7	63	5.5	104	6
#3	SPATA5	C9JT97	76	5.6	94	7
#4	skin aspartic protease	Q53RT3	37	5.3	610	0.1
#5	beta actin variant	P60709	42	5.3	99	15
#6	TRAIL-R2	O14763	48	5.4	100	18
#7	Cytokeratin-18	P05783	48	5.3	99	12
#8	TRAIL-R2	O14763	48	5.4	95	16
#9	RREB1	Q92766	52	5.3	109	10
#10	Cytokeratin-7	P08729	51	5.4	126	23
#11	Cytokeratin-18	P05783	48	5.3	497	13
#12	Cytokeratin-7	P08729	51	5.4	122	24
#13	FLJ31438	Q96N41	53	5.5	126	35
#14	Cytokeratin-7	P08729	51	5.4	406	36
#15	PAK65	Q13177	55	5.7	677	8
#16	Cytokeratin 8	P05787	54	5.5	694	32
#17	Cytokeratin 8	P05787	54	5.5	1143	72
#18	XRN1	Q8IZH2	54	5.8	353	8
#19	Jerky protein homolog-like	Q9Y4A0	51	6.0	130	22
#20	Eph receptor A10	Q5JZY3	32	5.7	119	9
#21	Glutathione S-transferase P	P09211	23	5.4	119	0.02

Table 2
Enrichment and isolation of antibodies to 2D-DIGE spots from non-immune libraries.

Spot	Protein name	Output/Input Ratio ($\times 10^{-7}$)/round				The number of isolated mAb.
		1st	2nd	3rd	4th	
#1	splicing factor YT521-B	6	7	16	480	4
#2	IkappaBR	6	7	15	500	3
#3	SPATA5	5	6	32	860	2
#4	skin aspartic protease	5	6	5	24	1
#5	beta actin variant	7	11	17	480	1
#6	TRAIL-R2	6	7	25	420	5
#7	Cytokeratin 18	5	11	62	260	4
#8	TRAIL-R2	5	27	41	1500	5
#9	RREB1	8	9	14	370	7
#10	Cytokeratin 7	6	7	3	2200	5
#11	Cytokeratin 18	6	8	15	84	2
#12	Cytokeratin 7	10	11	13	94	2
#13	FLJ31438	7	9	32	80	6
#14	Cytokeratin 7	4	7	46	280	5
#15	PAK65	7	11	51	580	9
#16	Cytokeratin 8	8	7	16	4100	6
#17	Cytokeratin 8	5	12	33	240	2
#18	XRN1	6	20	18	200	1
#19	Jerky protein homolog-like	7	10	49	940	3
#20	Eph receptor A10	8	6	57	3000	2
#21	Glutathione S-transferase P	7	8	110	1900	2

4. Discussion

Here, we aimed to develop a method of efficiently screening tumor-related biomarker proteins by proteome analysis. In

Table 3
Positive rate of identified proteins in breast cancer and normal breast tissues.

Protein name	Positive rate of antigens			
	Normal breast tissues		Breast cancer tissues	
Her-2	0/15	(0%)	53/189	(28%)
IkappaBR	3/15	(20%)	22/189	(12%)
SPATA5	0/15	(0%)	0/189	(0%)
beta actin variant	0/15	(0%)	0/189	(0%)
TRAIL-R2	0/15	(0%)	119/189	(63%)
RREB1	1/15	(7%)	83/189	(44%)
FLJ31438	0/15	(0%)	0/189	(0%)
PAK65	0/15	(0%)	0/189	(0%)
Cytokeratin 8	0/15	(0%)	137/189	(73%)
XRN1	0/15	(0%)	0/189	(0%)
Jerky protein homolog-like	0/15	(0%)	0/189	(0%)
Eph receptor A10	0/15	(0%)	93/189	(49%)

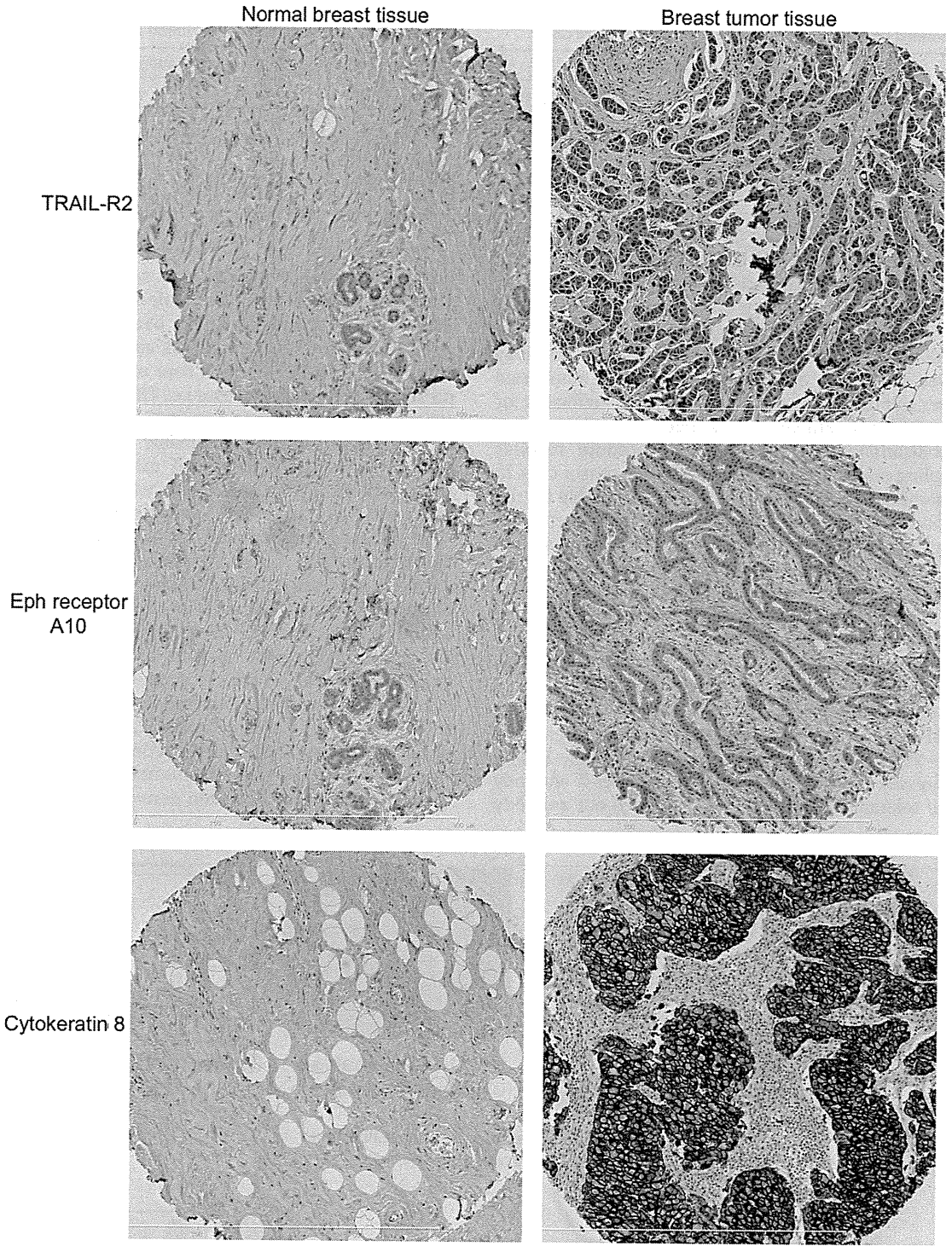

Fig. 3. Immunohistochemical staining of breast tumor and normal breast tissue microarray by scFv antibody-expressing phages. Typical images of breast cancer and normal breast tissue microarray stained by using scFv antibody-expressing phages to TRAIL-R2, Eph receptor A10 and Cytokeratin 8 are shown. Left panels are normal breast tissues and right panels are breast tumors. The tissue microarrays were counterstained by hematoxylin.

particular, we attempted to establish a means of isolating specific antibodies directly from small amounts of differentially expressed proteins obtained *via* 2D-DIGE analysis. To achieve this, we focused on a non-immune scFv phage library. Because the non-immune naïve scFv phage library has a huge repertoire of scFv on the surface of the phages, monoclonal antibodies to every antigen could be effectively isolated *in vitro*. Generally the diversity of the CDR3 domain, which is important for antigen-binding specificity, is estimated to be approximately twenty million [23]. Thus we reasoned that our previously constructed library, containing 2.4×10^9 scFv variants, has almost equal potential as the murine or human immune system [22]. Initially, in order to isolate monoclonal antibodies against very small amounts of antigen (hundreds of nanograms) recovered from the spots of 2D-DIGE analysis, we attempted to optimize the panning method using either a BIAcore® or nitrocellulose membrane. In the method using BIAcore®, the

Table 4
Positive rate of identified proteins in Her-2 positive and Her-2 negative cases.

Protein name	Positive rate of antigens in Her-2	
	Positive cases	Negative cases
TRAIL-R2	41/53 (77%)	78/136 (57%)
Cytokeratin 8	41/53 (77%)	91/136 (67%)
Eph receptor A10	33/53 (62%)	60/136 (44%)
TRAIL-R2 or Eph receptor A10	46/53 (87%)	100/136 (74%)

Table 5
Positive rate of identified proteins in clinical stage.

Protein name	Positive rate of antigens in clinical stage					
	Stage I		Stage II		Stage III	
Her-2	6/14	(43%)	17/87	(20%)	30/86	(35%)
TRAIL-R2	11/14	(79%)	51/87	(59%)	55/86	(64%)
Cytokeratin 8*	7/14	(50%)	58/87	(67%)	71/86	(83%)
Eph receptor A10*	4/14	(29%)	42/87	(48%)	47/86	(55%)

Man Whitney U test $^*P < 0.05$

enrichment of the desired clones was observed when immobilizing 5000 ng of KDR. By contrast, membrane-based panning led to the successful enrichment of clones from only 0.5 ng of KDR (Fig. 1). BIAcore-based panning has been recognized to be an effective method because the interaction of an antigen and a scFv antibody can be monitored in real time and the operation can be automated [24,25]. However, our results suggest that BIAcore® is inefficient for immobilizing very small amounts of antigen. This is because antigen immobilization using the BIAcore procedure requires a chemical coupling reaction with the surface of the sensor chip. In contrast, the membrane-based panning method is suitable for the isolation of antibodies against very small amounts of antigens. The suitability of this procedure when handling such small amounts of proteins presumably arises from the high efficiency of adsorption of antigens by the nitrocellulose membrane. These results show that monoclonal antibodies can be created from small amounts of proteins recovered from 2D-DIGE spots.

In breast cancer patients, the antibody targeting human epidermal growth factor receptor II (Her-2), is an effective drug [26,27]. However, because this receptor is over-expressed in only ~25% of breast cancer patients, anti-Her-2 antibody therapy is ineffective in ~75% of cases. Furthemore, approximately 30% of Her-2 over-expressed patients that received anti-Her-2 antibody therapy became tolerant [28–30]. Thus, we applied our antibody proteomics system to breast cancer samples for identification of the proteins to replace Her-2 as suitable therapeutic targets. Initially, 21 differentially expressed proteins between SKBR3 and 184A1 cells were found by 2D-DIGE analysis and 16 different proteins were identified by MALDI-TOF/MS. Four of the identified proteins were present in more than one spot i.e., TRAIL-R2 (spot 6, 8), Cytokeratin 18 (spot 7, 11), Cytokeratin 8 (spot 16, 17) and Cytokeratin 7 (spot 10, 12, 14). These proteins presumably display different pI and MW values due to posttranslational modification. Next, membrane-based panning against these spots was performed, and the output/input ratio of phage titer after the fourth round of panning increased from approximately 20-fold–4000-fold in comparison to that after the first round of panning. Moreover, we screened scFv antibody-expressing phages binding to each spot protein by phage ELISA and obtained each spot-specific scFv antibodies from all spots after approximately two weeks. Finally, it was necessary to select the most valuable proteins from a large number of differentially expressed proteins in breast cancer cells. Using the isolated spot-specific scFv antibody-expressing phages, we immunostained a TMA with 189 cases of breast cancer tissue and 15 samples of normal tissue. SPATA5, Beta actin, FLJ31438, PAK65 and XRN1 were not detected in either the tumor tissue or normal tissue. Thus, these proteins may have been derived from cell lines used in the

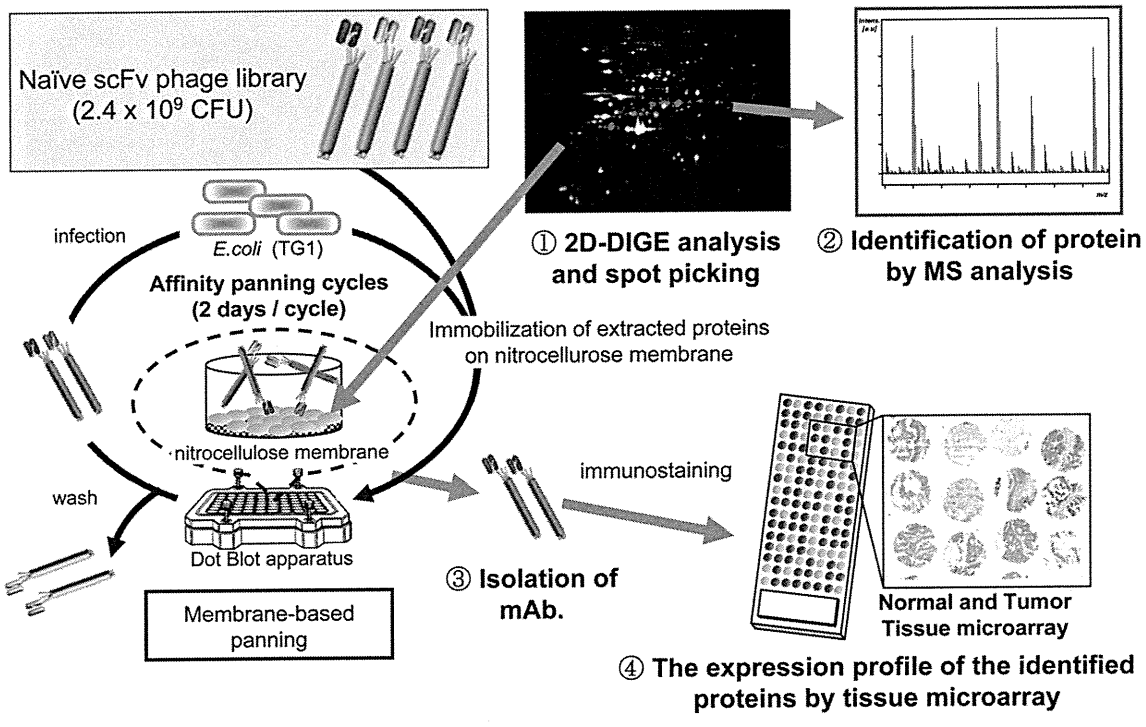

Fig. 4. Schematic illustration of the antibody proteomics system. Antibody proteomics system is an efficient method for screening tumor-related biomarker proteins. Because this system involves the direct isolation of monoclonal antibodies from 2D-DIGE spots without preparation of recombinant proteins, it enables the discovery and validation of tumor-related biomarker proteins by TMA analysis using the isolated scFv antibody-expressing phages.

proteome analysis or the antibodies against these proteins may not detect the antigen on formalin-fixed paraffin-embedded tissues. By contrast, TRAIL-R2, Cytokeratin 8 and Eph receptor A10 were specifically-expressed in over 40% of breast cancer tissues. We confirmed the immunohistochemical staining image generated by scFv antibody-expressing phages displayed a similar pattern to that generated by IgG type commercial antibody (data not shown). Interestingly, the expression rates of TRAIL-R2, Cytokeratin 8 and Eph receptor A10 were higher than the existing breast cancer marker, Her-2 (only about 25%). Moreover, the expression rates of TRAIL-R2 and Eph receptor A10 (cell membrane proteins) in Her-2 negative cases were over 40% and in Her-2 positive cases over 60%. This data indicates that TRAIL-R2 and Eph receptor A10 are promising alternative target candidates for anti-Her-2 antibody therapy ineffective patients, at least in terms of the expression profile. Further work is required to analyze the function of these proteins in more detail. Furthermore, by checking antigen expression profiles against clinical information, the expression rate of Cytokeratin 8 and Eph receptor A10 was found to have increased during progression of the clinical symptoms. These observations indicate that Cytokeratin 8 and Eph receptor A10 are promising diagnostic marker candidates for assessing the aggressiveness of breast cancer.

Recently, an anti-TRAIL-R2 antibody has been developed as an anticancer drug [31–33]. Moreover, Cytokeratin 8 has gained considerable attention as a cancer aggressiveness diagnostic marker [34–36]. These results demonstrate that this technology is able to select well-known drug-target markers (i.e., TRAIL-R2) and diagnostic markers (i.e., Cytokeratin 8) as well as unknown biomarker protein candidates (Eph receptor A10) from a large variety of differentially expressed proteins in cancer cells.

Our method employs a set of techniques for efficiently identifying biomarker candidates. Specifically, the method entails; 1) searching for differentially expressed proteins in disease samples, 2) identification of the proteins, 3) high throughput isolation of monoclonal antibodies against the proteins using a naïve scFv phage library, and 4) validation of the proteins by TMA analysis. This methodology is referred to as an "antibody proteomics system" (Fig. 4). We believe that the proteins identified using this approach will contribute to the drug development process. Indeed, the antibody proteomics system could become a platform technology for seeking tumor-related biomarker proteins by a proteomics-based approach.

5. Conclusions

In this study, we established the antibody proteomics system for efficiently screening and validating tumor-related biomarker proteins of interest by isolating specific antibodies directly from small amounts of proteins obtained *via* 2D-DIGE analysis. Applying this technique to the identification of breast tumor-related biomarker proteins, the expressions of Eph receptor A10, TRAIL-R2 and Cytokeratin 8 in breast tumor tissues were successfully validated from a large number of candidates. These results demonstrate that our original technology is an efficient and useful method for screening tumor-related biomarker proteins. Moreover, Eph receptor A10, TRAIL-R2 and Cytokeratin 8 identified in this study are promising breast tumor biomarkers for drug development.

Acknowledgement

We thank Dr. Junya Fukuoka, Department of Surgical Pathology, Toyama University Hospital, for valuable advice during our pathological analysis.

This study was supported in part by Grants-in-Aid for Scientific Research from the Ministry of Education, Culture, Sports, Science and Technology of Japan, and from the Japan Society for the Promotion of Science (JSPS). This study was also supported in part by Health Labour Sciences Research Grants from the Ministry of Health, Labor and Welfare of Japan, and by Health Sciences Research Grants for Research on Publicly Essential Drugs and Medical Devices from the Japan Health Sciences Foundation.

Appendix

Figure with essential color discrimination. Figs. 2–4 in this article have parts that are difficult to interpret in black and white. The full color images can be found in the on-line version, at doi:10.1016/j.biomaterials.2010.09.030.

References

[1] Hanash S. Disease proteomics. Nature 2003;422(6928):226–32.
[2] Kavallaris M, Marshall GM. Proteomics and disease: opportunities and challenges. Med J Aust 2005;182(11):575–9.
[3] Oh-Ishi M, Maeda T. Disease proteomics of high-molecular-mass proteins by two-dimensional gel electrophoresis with agarose gels in the first dimension (Agarose 2-DE). J Chromatogr B Analyt Technol Biomed Life Sci 2007;849 (1–2):211–22.
[4] Chaga GS. Antibody arrays for determination of relative protein abundances. Methods Mol Biol 2008;441:129–51.
[5] Kaufmann H, Bailey JE, Fussenegger M. Use of antibodies for detection of phosphorylated proteins separated by two-dimensional gel electrophoresis. Proteomics 2001;1(2):194–9.
[6] Xu ZW, Zhang T, Song CJ, Li Q, Zhuang R, Yang K, et al. Application of sandwich ELISA for detecting tag fusion proteins in high throughput. Appl Microbiol Biotechnol 2008;81(1):183–9.
[7] Au NH, Gown AM, Cheang M, Huntsman D, Yorida E, Elliott WM, et al. P63 expression in lung carcinoma: a tissue microarray study of 408 cases. Appl Immunohistochem Mol Morphol 2004;12(3):240–7.
[8] de Jong D, Xie W, Rosenwald A, Chhanabhai M, Gaulard P, Klapper W, et al. Immunohistochemical prognostic markers in diffuse large B-cell lymphoma: validation of tissue microarray as a prerequisite for broad clinical applications (a study from the Lunenburg Lymphoma Biomarker Consortium). J Clin Pathol 2009;62(2):128–38.
[9] Kozarova A, Petrinac S, Ali A, Hudson JW. Array of informatics: applications in modern research. J Proteome Res 2006;5(5):1051–9.
[10] Rimm DL, Camp RL, Charette LA, Costa J, Olsen DA, Reiss M. Tissue microarray: a new technology for amplification of tissue resources. Cancer J 2001;7 (1):24–31.
[11] Tawfik El-Mansi M, Williams AR. Validation of tissue microarray technology using cervical adenocarcinoma and its precursors as a model system. Int J Gynecol Cancer 2006;16(3):1225–33.
[12] Asadi A, Pourfathollah AA, Mahdavi M, Eftekharian MM, Moazzeni SM. Preparation of antibody against horseradish peroxidase using hybridoma technology. Hum Antibodies 2008;17(3–4):73–8.
[13] Hadas E, Theilen G. Production of monoclonal antibodies. The effect of hybridoma concentration on the yield of antibody-producing clones. J Immunol Methods 1987;96(1):3–6.
[14] Makonkawkeyoon L, Pharephan S, Makonkawkeyoon S. Production of a mouse hybridoma secreting monoclonal antibody highly specific to hemoglobin Bart's (gamma4). Lab Hematol 2006;12(4):193–200.
[15] McKinney KL, Dilwith R, Belfort G. Optimizing antibody production in batch hybridoma cell culture. J Biotechnol 1995;40(1):31–48.
[16] Barbas 3rd CF, Kang AS, Lerner RA, Benkovic SJ. Assembly of combinatorial antibody libraries on phage surfaces: the gene III site. Proc Natl Acad Sci U S A 1991;88(18):7978–82.
[17] Coomber DW. Panning of antibody phage-display libraries. Standard protocols. Methods Mol Biol 2002;178:133–45.
[18] McCafferty J, Griffiths AD, Winter G, Chiswell DJ. Phage antibodies: filamentous phage displaying antibody variable domains. Nature 1990;348 (6301):552–4.
[19] Okamoto T, Mukai Y, Yoshioka Y, Shibata H, Kawamura M, Yamamoto Y, et al. Optimal construction of non-immune scFv phage display libraries from mouse bone marrow and spleen established to select specific scFvs efficiently binding to antigen. Biochem Biophys Res Commun 2004;323 (2):583–91.
[20] Smith GP. Filamentous fusion phage: novel expression vectors that display cloned antigens on the virion surface. Science 1985;228(4705):1315–7.
[21] Vaughan TJ, Williams AJ, Pritchard K, Osbourn JK, Pope AR, Earnshaw JC, et al. Human antibodies with sub-nanomolar affinities isolated from a large non-immunized phage display library. Nat Biotechnol 1996;14(3):309–14.